NATIONAL COOPERATIVE HIGHWAY RESEARCH PROGRAM
REPORT 97

ANALYSIS OF STRUCTURAL BEHAVIOR OF AASHO ROAD TEST RIGID PAVEMENTS

HIGHWAY RESEARCH BOARD
NATIONAL RESEARCH COUNCIL
NATIONAL ACADEMY OF SCIENCES—NATIONAL ACADEMY OF ENGINEERING

NATIONAL COOPERATIVE HIGHWAY RESEARCH PROGRAM
REPORT 97

ANALYSIS OF STRUCTURAL BEHAVIOR OF AASHO ROAD TEST RIGID PAVEMENTS

ALEKSANDAR S. VESIC AND SURENDRA K. SAXENA
DUKE UNIVERSITY
DURHAM, NORTH CAROLINA

RESEARCH SPONSORED BY THE AMERICAN ASSOCIATION
OF STATE HIGHWAY OFFICIALS IN COOPERATION
WITH THE BUREAU OF PUBLIC ROADS

SUBJECT CLASSIFICATIONS
PAVEMENT DESIGN
PAVEMENT PERFORMANCE
FOUNDATIONS (SOILS)
MECHANICS (EARTH MASS)

HIGHWAY RESEARCH BOARD
DIVISION OF ENGINEERING NATIONAL RESEARCH COUNCIL
NATIONAL ACADEMY OF SCIENCES—NATIONAL ACADEMY OF ENGINEERING 1970

NATIONAL COOPERATIVE HIGHWAY RESEARCH PROGRAM

Systematic, well-designed research provides the most effective approach to the solution of many problems facing highway administrators and engineers. Often, highway problems are of local interest and can best be studied by highway departments individually or in cooperation with their state universities and others. However, the accelerating growth of highway transportation develops increasingly complex problems of wide interest to highway authorities. These problems are best studied through a coordinated program of cooperative research.

In recognition of these needs, the highway administrators of the American Association of State Highway Officials initiated in 1962 an objective national highway research program employing modern scientific techniques. This program is supported on a continuing basis by funds from participating member states of the Association and it receives the full cooperation and support of the Bureau of Public Roads, United States Department of Transportation.

The Highway Research Board of the National Academy of Sciences-National Research Council was requested by the Association to administer the research program because of the Board's recognized objectivity and understanding of modern research practices. The Board is uniquely suited for this purpose as: it maintains an extensive committee structure from which authorities on any highway transportation subject may be drawn; it possesses avenues of communications and cooperation with federal, state, and local governmental agencies, universities, and industry; its relationship to its parent organization, the National Academy of Sciences, a private, nonprofit institution, is an insurance of objectivity; it maintains a full-time research correlation staff of specialists in highway transportation matters to bring the findings of research directly to those who are in a position to use them.

The program is developed on the basis of research needs identified by chief administrators of the highway departments and by committees of AASHO. Each year, specific areas of research needs to be included in the program are proposed to the Academy and the Board by the American Association of State Highway Officials. Research projects to fulfill these needs are defined by the Board, and qualified research agencies are selected from those that have submitted proposals. Administration and surveillance of research contracts are responsibilities of the Academy and its Highway Research Board.

The needs for highway research are many, and the National Cooperative Highway Research Program can make significant contributions to the solution of highway transportation problems of mutual concern to many responsible groups. The program, however, is intended to complement rather than to substitute for or duplicate other highway research programs.

NCHRP Report 97

Project 1-4(1)A FY '64
SBN 309-01884-6
L C. Card No. 74-606601

Price: $2.60

Published reports of the

NATIONAL COOPERATIVE HIGHWAY RESEARCH PROGRAM

are available from:

Highway Research Board
National Academy of Sciences
2101 Constitution Avenue
Washington, D.C. 20418

(See last pages for list of published titles and prices)

FOREWORD

By Staff

Highway Research Board

This report will be of interest to highway engineers and researchers involved in rigid pavement design. It examines existing theories of structural behavior of rigid pavements and analyzes data from the AASHO Road Test as they apply to the observed behavior of the pavements. The analysis indicates that existing mechanistic theories are generally adequate for use in the design of rigid highway pavements, and that the very large number of load applications to which pavements are now being subjected has a significant influence on rigid pavement performance. The report also contains suggestions for further research and field observations for verification and modification of parameter values used in design.

The present state of the art in the area of rigid pavement design is to a large degree based on experience gained by trial and error and empirical relationships developed during field experiments such as the AASHO Road Test. As long as the designer is dealing with foundation soils, environmental factors, material properties, construction techniques, and traffic loading conditions that are similar to those for which the relationships have been determined, the performance can be reasonably well predicted. However, as design parameters change a need exists for a more rational approach to pavement design.

The objective of this study was to examine existing theories for structural behavior of rigid pavements in view of the large amount of controlled field performance data collected during the Road Test. A most significant contribution of the study toward the ultimate solution to the problem is the development of a relationship between tensile stress in the pavement slab caused by moving loads and portland cement concrete pavement performance. This lends support to most existing theoretical methods of rigid pavement design. It will be of particular value to highway engineers faced with the problem of designing rigid pavements for rapidly increasing traffic, heavier wheel loads, and new or modified materials and construction techniques.

The evidence of the relationship between traffic loadings and concrete slab strength and thickness is so strong—based on pavement slabs of 2.5- to 11-in. thickness and single-axle loadings of 6,000 to 30,000 lb—that the findings should have some direct practical application without the need for confirmation by further research or translation into specifications or standards. The equation expressing the relationship provides an opportunity for quantitative evaluation of the effect of variations in strength and slab thickness on pavement performance and thus strongly supports the need for quality control during construction. The expression also offers an adequate rational basis for evaluation of an equivalent number of axle load applications for rigid pavements subjected to mixed traffic. In addition to the previously described potential for practical application, the research findings contribute substantially to the progress being made in the area of more rational approaches to structural design of pavements. Using existing mechanistic theories, designers responsible for specialized problems not easily solved by normal procedures should be able, by utilizing the results of this study, to predict with more certainty the potential life of a rigid pavement.

CONTENTS

ACKNOWLEDGMENTS

The investigations reported in this study were performed in the Department of Civil Engineering, Duke University, with Aleksandar S. Vesić, Professor of Civil Engineering, as Principal Investigator. The report covers the second phase of NCHRP Project 1-4(1), entitled "Extension of Road Test Performance Concepts." The report on the first phase of this project, dealing with structural behavior of flexible pavements, has been published as *NCHRP Report 10*.

This report was written by Dr. Vesić. The Appendix was prepared by Surendra K. Saxena, Research Assistant, who was in charge of the numerical evaluation of stresses and deflections in pavement slabs which formed the basis for the presented analyses. In this work they were assisted by Rajendra S. Bhatnagar, Research Assistant.

ANALYSIS OF STRUCTURAL BEHAVIOR OF AASHO ROAD TEST RIGID PAVEMENTS

SUMMARY

Chapter One is devoted to a critical review of existing theories of structural behavior of rigid pavements. These theories differ principally in the model selected to represent the subgrade supporting the pavement slab. The two principal models currently used are (a) the elastic-isotropic solid, characterized by a modulus of deformation, E_s, and a Poisson's ratio, ν_s; and (b) the Winkler subgrade, characterized by a coefficient of subgrade reaction, k.

It is shown that, with a suitable selection of coefficient k, theories based on the Winkler model for the subgrade can furnish adequate answers also for slabs resting on a subgrade behaving as an elastic solid. However, there is no single value of k that can give perfect agreement of all statical influences in a particular case, unless the subgrade thickness is limited to a maximum of 2.5 stiffness radii of the slab. Simple analytical expressions for evaluation of k in terms of known characteristics of the slab and the subgrade are presented.

Chapter Two is devoted to a study of structural behavior of rigid pavements of the AASHO Road Test. It is shown that the over-all response of the AASHO subgrade to loads is comparable to response of an ideal isotropic-elastic solid. However, with proper selection of the coefficients of subgrade reaction, k, the Winkler subgrade model (used in the well-known Westergaard theory of rigid pavements) can also lead to good predictions of pavement stresses and deflections. The coefficient k for the AASHO pavement/subgrade systems is a variable quantity, which is inversely proportional to the pavement slab thickness.

It is also demonstrated that the combined tensile stress in pavement slabs represents the best indicator of pavement performance. A simple expression relating the ultimate number of axle-load applications to the flexural strength of the pavement material, the thickness of the pavement slab, and the magnitude of the axle load is derived, indicating that the pavement life should be proportional to the fourth power of strength and to the fifth power of slab thickness and inversely proportional to the fourth power of the axle load. This expression offers for the first time a rational basis for evaluation of equivalent number of axle-load applications for rigid pavements subjected to mixed traffic.

CHAPTER ONE

INTRODUCTION AND THEORETICAL CONSIDERATIONS

The aim of this study is to provide a rational, mechanistic interpretation of measurements and observations made on rigid pavements during the AASHO Road Test. The work has been initiated by the American Association of State Highway Officials through the National Cooperative Highway Research Program in the desire of preparing a sound theoretical basis for translation of AASHO Road Test results into other ambient conditions.

Although the study treats all the major aspects of structural behavior of rigid pavements, it is centered around two principal indicators of rigid pavement performance—namely, stresses in the pavement slabs and pavement deflections under load. Attention is also given to the patterns of slab cracking and failure under the vehicular traffic.

This first chapter is devoted to a critical review of existing theories of structural behavior of rigid pavements, with particular emphasis to the meaning and evaluation of coefficient of subgrade reaction, k Chapter Two describes assembled data on measured strains and deflections of pavement slabs, as well as on deformation characteristics of pavement materials and subgrade soils. Finally, Chapters Three and Four contain analyses of assembled information, appraisals of the meaning and value of findings of the present study, and recommendations for future research on mechanics of rigid pavements.

EXISTING THEORIES OF STRUCTURAL BEHAVIOR OF RIGID PAVEMENTS

The first attempt at a rational approach to rigid pavement design was recorded in the literature about 1920, when the so-called "corner formula" for stresses in a concrete slab was proposed (*1, 2*). This formula was based on the assumption that the slab corner acts as a cantilever beam of variable width, receiving no support from the subgrade between the corner and the point of maximum moment in the slab. Although the observations in the first road test with rigid pavements (*3*) seemed to be in agreement with the predictions of this formula, its use remained, for obvious reasons, very limited.

The first complete theory of structural behavior of rigid pavements was that developed by Westergaard in the 1920's (*4, 5*) by extension of the classical Hertz solution for stresses in a floating slab (*6*). This well-known theory considers the pavement to act as a homogeneous, isotropic, elastic, thin slab resting on an ideal subgrade that exerts, at any point, a vertical reactive pressure, p, proportional to the deflection, w, of the slab at the same point (Winkler subgrade). The constant of proportionality

$$p/w = k \qquad (1)$$

which is a quantity of dimension FL^{-3}, is called "coefficient of subgrade reaction." According to the physical interpretation of Eq. 1, the subgrade should react as a bed of springs having a spring constant equal to k, or as a heavy liquid of density k.

Extensive investigations of structural behavior of concrete pavement slabs performed in the 1930's at the Arlington (Va.) Experimental Farm (*7*) and at Iowa State Engineering Experiment Station (*8, 9*) showed, basically, good agreement between observed stresses and those computed by the Westergaard theory, as long as the slab remained continuously supported by the subgrade. Corrections were proposed only for the Westergaard corner formula (*9, 10*) to take care of the effects of slab curling on subgrade support However, although a proper choice of the coefficient of subgrade reaction was found to be essential for good agreement, there remained much ambiguity in the methods for experimental determination of that coefficient.

During the same period, a considerable amount of experimental evidence was assembled, indicating that the behavior of many subgrades may be closer to that of elastic, isotropic (Hookean) solids, defined by two deformation characteristics such as a modulus of deformation, E_s, and a Poisson's ratio, ν_s. Based on this concept of subgrade, and assuming that the pavement slab also acts as an elastic solid layer of infinite extent and finite thickness, Burmister proposed in 1943 (*11*) his layered solid theory of structural behavior of rigid pavements. He suggested that the design should be based on a criterion of limited deformation under load. However, the design procedures for rigid pavements based on his theory were never developed to the extent needed for regular use in engineering practice. In this respect the lack of analogous solutions for pavement slabs of finite extent (edge and corner case) was of particular disadvantage

Other approaches based on the assumption that the subgrade behaves as an elastic-isotropic solid have been developed by Odemark (*12*), Pickett and Ray (*13*), Peltier (*14*), Jeuffroy (*15*), and others. These approaches use as their basis a solution by Holl (*16*) and Hogg (*17*) of the problem of a thin elastic slab of infinite extent resting on an elastic-isotropic solid. Most of these approaches retain, however, as the principal design criterion, the condition that the tensile stress in the pavement slab should remain within certain limits governed by the tensile strength of the slab material in bending.

All the preceding theories and approaches are concerned with structural behavior of rigid pavement systems in the range of working stresses, where deflections, by assumption, are proportional to applied loads. Following the development of the yield-line theory of slabs (*18*), an ultimate-strength theory of rigid pavement design was proposed by Losberg (*19*). The basic philosophy of this theory is similar to that of the theory of plastic design of steel struc-

tures: the slab is considered to be at the verge of yield or fracture. In this condition it is possible to evaluate the unknown statical influences, such as bending moments and shearing forces, along an assumed continuous yield (crack) pattern from considerations of ultimate strength of the pavement slab material. The ultimate load on the slab is then determined from considerations of static equilibrium of an isolated portion of the slab, bound by a continuous yield line (crack). For such an evaluation it is necessary to introduce also some distribution of the reactive pressure of the subgrade against the slab. In the Losberg theory this is done by assuming that at the instant of slab failure the subgrade reacts as a Winkler subgrade while the slab bound by the yield line still behaves as a thin, elastic slab.

All the existing theories can be grouped according to models used to simulate the pavement and subgrade behaviors, as given in Table 1. Three different models are used for the pavement slab—elastic-isotropic solid, thin elastic slab, and thin elastic-plastic slab. Two different models are used for the subgrade—elastic-isotropic solid, and Winkler subgrade.

A relatively brief analysis is needed to show that the differences in stress and deflection patterns between the three pavement slab models mentioned are nominal, as long as one is dealing with stresses imposed by vertical pavement loads, and as long as the usual corrections for thick-slab effects in the immediate vicinity of the loaded area are introduced. This is shown in Figure 1, which was prepared by using some stress analyses based on the Burmister two-layered solid theory (*20*). The upper part of this figure shows the variation of vertical stress, σ_z, with depth as a function of the ratio of the deformation moduli of the two layers, E_1/E_2, for a rough interface (solid lines) and a smooth interface (dashed lines) between two layers. The lower part of the figure shows the variation of the radial stress, σ_r, under the center of the loaded area, again as a function of the moduli ratio, E_1/E_2 Inasmuch as the typical moduli ratios for rigid pavements are rarely smaller than 100, the data in the figure indicate beyond doubt that the Navier hypothesis of plane sections and stresses proportional to distance from the neutral axis (fundamental for the thin-slab analysis) is close to being satisfied, at least for typical concrete pavements.

Consequently, in any attempt to make an appraisal of different theories of structural behavior of rigid pavements major attention should be devoted to the evaluation of models proposed for the pavement subgrade. Particularly intriguing is the Winkler model of a subgrade characterized by a coefficient of subgrade reaction, k, as defined by Eq. 1. As indicated earlier, most of the currently used theoretical design methods for rigid pavements use the Winkler model, and a number of investigators report good agreement between the observed response of rigid pavements and the predictions made on the basis of that model. At the same time there exists ample evidence that the elastic-isotropic solid model can, in general, predict more closely the response of real soils to load.

A possible explanation of this apparent controversy should be sought before making any attempts at a rational interpretation of the AASHO Road Test data. With this purpose in mind, the following section discusses the meaning of the coefficient of subgrade reaction, k, in the analysis of slabs resting on soil.

TABLE 1

EXISTING THEORIES OF STRUCTURAL BEHAVIOR OF RIGID PAVEMENTS

SLAB MODEL \ SUBGRADE MODEL	ELASTIC-ISOTROPIC SOLID	WINKLER SUBGRADE
Elastic-isotropic solid	Burmister (1943)	———
Thin, elastic slab	Hogg (1938) Holl (1938) Pickett and Ray (1951)	Westergaard (1925, 1927)
Thin, elastic-plastic slab	———	Losberg (1960)

THE MEANING OF COEFFICIENT k

When Winkler first introduced his assumption that $p = kw$ for analysis of a beam resting on soil (*21*), he did not say anything about the coefficient, k. Twenty years later Zimmerman (*22*), in his treatise on the analysis of railway ties and rails, defined k as a constant depending on the type of subgrade. During the subsequent development of theory of

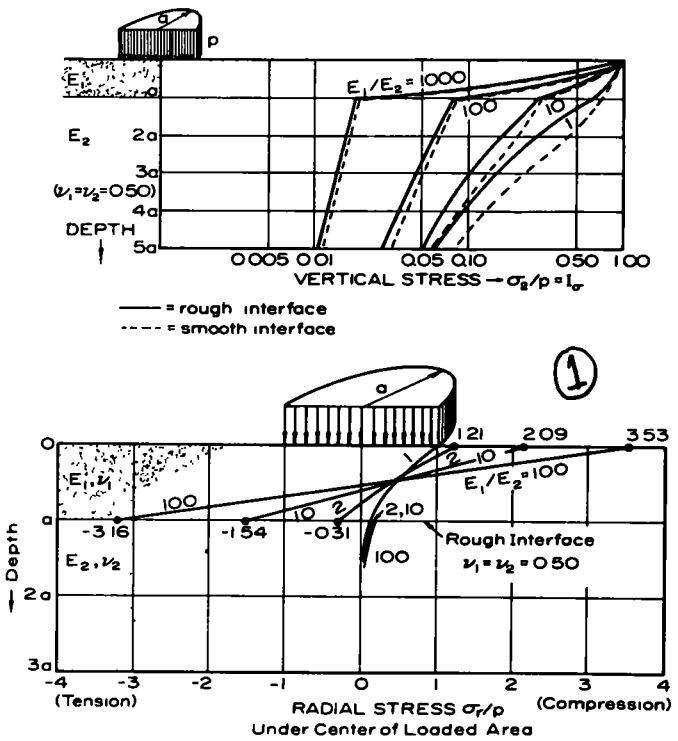

Figure 1. Variation of vertical and radial stresses in a two-layered solid.

beams and slabs resting on soil this concept prevailed, although many early investigators recognized that k was a quantity depending also on the size and shape of the loaded area (*23, 24*).

In his first paper on theoretical analysis of concrete pavements (*4*) Westergaard recognized the lack of a consistent method of predetermination of k. As a consolation he presented the often repeated statement that larger variations in coefficient of subgrade reaction have only a minor effect on computed stresses. He finally suggested that this coefficient may best be determined by comparing the deflections of full-sized slabs with deflections given by his formulas. Nevertheless, in subsequent development of his design method most investigators preferred to determine k from plate load tests. Because the Arlington tests (*7*) indicated little reduction in k beyond plate diameters of 30 in., a number of agencies have adopted the circular rigid plate of that size as the standard plate for determination of k. In this way k remained in pavement design as a quantity depending on the properties of the subgrade only.

In the meantime, developments in the field of soil mechanics have increasingly pointed out the inadequacy of the Winkler model for simulation of soil response to load in general (*25*). Biot (*26*) found a solution of the problem of bending of an infinite beam resting on an elastic-isotropic solid and demonstrated that k should depend on the size, shape, and structural stiffness of the beam, as well as on the deformation properties of the soil By 1950 a number of investigators recommended abandoning completely the coefficient k and all the theories based on it (*27, 28*).

In 1955 Terzaghi published a paper (*29*) in which he reviewed the entire history and development of theories based on the coefficient k and pleaded for the right place of these theories in the engineering practice. He contended that although the Winkler model was artificial and had little to do with the actual response of soils to load, the theories based on it still can give reasonable estimates of bending moments or stresses in beams and slabs, provided the right value of k can be selected. He suggested, however, that no agreement of deflections should be expected from similar analyses. He recommended that the k-value for slabs on soil be determined by extrapolating the results of load tests on a 12-in.-diameter plate to the range of influence of the load acting on the slab, which he defined as equal to 2.5 stiffness radii of the slab.

In 1961, after extending Biot's theory of bending of beams resting on an elastic-isotropic solid, Vesić (*30*) showed that it was possible to select a value of k so as to obtain a good approximation of both bending moments and deflections of a beam resting on a solid, provided the beam is sufficiently long. For a beam of width B and structural stiffness $E_b I$, resting on a solid whose deformation characteristics are E_s and ν_s, this value of k is given by

$$k B = K = 0.65 \sqrt[12]{\frac{E_s B^3}{E_b I}} \frac{E_s}{1 - \nu_s^2} \tag{2}$$

in which the quantity $kB = K$ (in tons/ft^2) is called modulus of subgrade reaction. Further investigations (*31, 32*) confirmed experimentally that it was possible to predetermine the k-values of beams resting on soil by using Eq. 2 and soil deformation characteristics E_s and ν_s obtained from triaxial and plate load tests.

As a result of all studies performed, the real meaning of the modulus of subgrade reaction *for beams* resting on soil emerges as follows. in analysis of flexible beams resting on soil it is justified to assume that the contact pressures per unit length of the beam are proportional to the deflections at the corresponding point. The constant of proportionality, K, expressed in stress units, increases directly with the plane-strain modulus of deformation of the subgrade, $E_s/1 - \nu_s^2$, as well as with the twelfth root of the relative flexibility of the beam with respect to the subgrade.

Of course, for the purpose of this investigation it is of the greatest interest to find out whether any similar statements can be made for a flexible *slab* resting on soil, and, if so, what value should be assigned to the coefficient of subgrade reaction, k.

COEFFICIENT OF SUBGRADE REACTION, k, FOR SLABS

In an attempt to answer these questions, consider a slab of infinite extent and thickness h, resting on a semi-infinite elastic-isotropic solid characterized by a modulus of deformation, E_s, and a Poisson's ratio, ν_s (Fig. 2). Under the action of a vertical point load, Q, the slab deflection at any point at distance r from the load will be (*16, 17*)

$$w = \frac{Q\, l_0^2}{2\pi D} \int_0^\infty \frac{J_0\,(\lambda r/l_0)\, d\lambda}{1 + \lambda^3} = \frac{P\, l_0^2}{D}\, I_w \tag{3}$$

in which l_0 is a characteristic length defined by

$$l_0 = \sqrt[4]{\frac{2D\,(1 - \nu_s^2)}{E_s}} \tag{4}$$

D is the flexural stiffness of the slab, defined by

$$D = \frac{E\, h^3}{12\,(1 - \nu^2)} \tag{5}$$

J_0 is the Bessel function of zero order and $\lambda = \alpha l_0$, where α is a parameter. Values of characteristic length l_0 for typical ranges of slab thicknesses h and subgrade moduli E_s are given in Table 2

Using the same notation the contact pressure distribution is found to be

$$p = \frac{Q}{2\pi\, l_0^2} \int_0^\infty \frac{J_0\,(\lambda r/l_0)\, \lambda\, d\lambda}{1 + \lambda^3} = \frac{Q}{l_0^2}\, I_p \tag{6}$$

The variation of the dimensionless deflection factor, I_w, and the pressure factor, I_p, with relative distance, r/l_0, from the load is shown in Figure 3a The ratio of pressure and deflection at the origin (under the load Q) is

$$\frac{p_{max}}{w_{max}} = \frac{D}{l_0^4} = k_0 \tag{7}$$

However, as the contact pressures decrease faster with distance than the deflections, the coefficient k decreases with distance, as shown in Figure 3b. By using the Hertz-Westergaard theory for the same case, with a constant

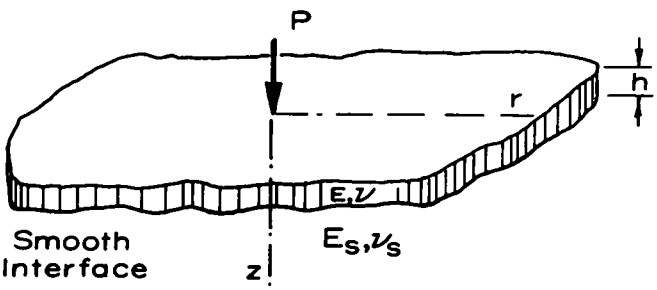

Figure 2. Slab of infinite extent resting on an elastic, isotropic solid

TABLE 2

TYPICAL VALUES OF CHARACTERISTIC LENGTH, l_o[a]

MODULUS OF DEFORMATION OF THE SOIL, E, (LB/IN.^{2})	CHARACTERISTIC LENGTH FOR SLAB THICKNESS, h, OF (IN.)		
	6 IN	9 IN.	12 IN.
1,000	30.5	45.8	61.2
10,000	14 2	21.2	28.4
100,000	6.6	8.1	10 8

[a] All values computed with the following deformation characteristic of concrete E_s=6,250,000 lb/in^2, ν_s=0 28

coefficient of subgrade reaction equal to k_0, one obtains relatively poor agreement of pressures and deflections This is evident in Figure 3a, where the corresponding variation of both pressure and deflection factors, I_p and I_w, with distance is shown by a dashed line.

To improve agreement of pressures according to the two compared theories one can select some other value of k. By taking a value $k_p = 2.37\ k_0$, which will make the maximum pressures under the load equal, a very good agreement of pressures can be obtained; however, the agreement of deflections will be even poorer than with $k = k_0$. On the other hand, one can select a value of $k_w = 0.42\ k_0$ so as to have the same maximum deflections under load, again with much poorer agreement of pressures. It may be concluded that, strictly speaking, *there is no single value of* k *that can yield agreement of all statical influences, such as pressures, shearing forces, bending moments, and deflections, across the slab.* In particular, the k-value obtained by comparing maximum deflections will be about 2.4 times lower than the k-value giving a good agreement of bending moments or stresses in the slab and six times lower than the k-value giving a good agreement of contact pressures between the slab and the supporting subgrade.

Timoshenko and Woinowsky-Krieger (*33*), in similar analyses, found that the bending moments in the vicinity of the load will be the same in both analyses if one selects $k = k_o$. This yields, from Eqs. 7 and 4, the following expression for the coefficient of subgrade reaction, k, of slabs resting on an isotropic-elastic solid:

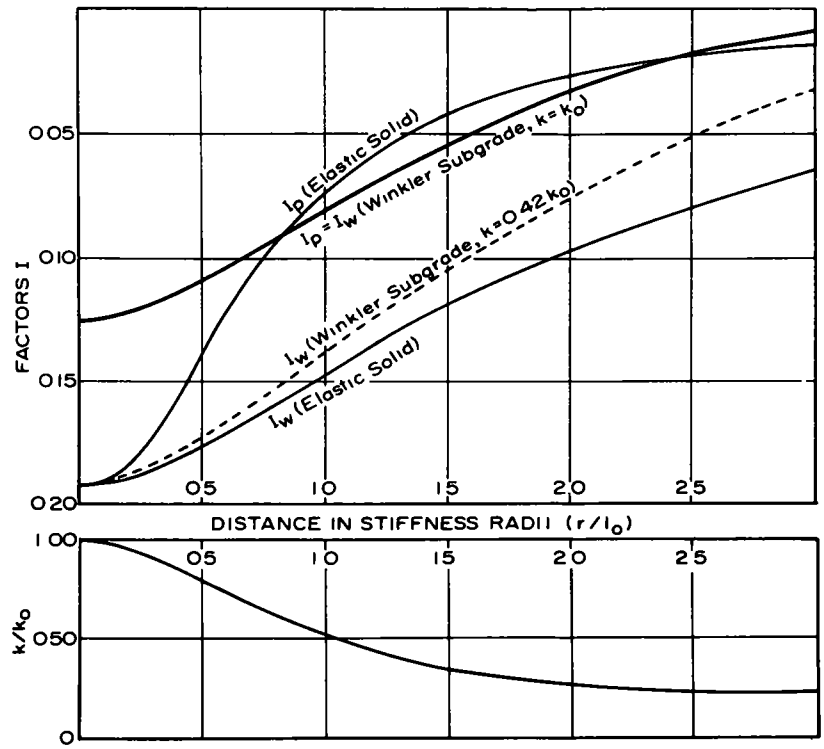

Figure 3. Variation of factors, I, *and coefficient,* k, *with relative distance,* r/l_o.

$$k = k_0 = 0.91 \sqrt[3]{\frac{E_s (1 - \nu^2)}{E (1 - \nu_s^2)}} \frac{E_s}{(1 - \nu_s^2) h} \quad (8)$$

This expression can be somewhat simplified by putting $\nu = 0.15$ and $\nu_s = 0.50$ in the term under the third root sign. In this way Eq. 8 is transformed into

$$k = k_0 = \sqrt[3]{\frac{E_s}{E}} \frac{E_s}{(1 - \nu_s^2) h} \quad (9)$$

which is, in some way, analogous to Eq 2 for beams. It indicates that the coefficient k for slabs is not a characteristic of the subgrade only it depends on the relative flexibility of the slab with respect to the subgrade. Most significantly, it indicates that, in a given location, such as the AASHO Road Test site, *the coefficient,* k, *should be inversely proportional to the thickness,* h, *of the pavement slabs.*

It may be added that, according to the preceding discussion, the k-value given by Eq. 9 should give good agreement of bending moments or stresses in the slab only. By using the same value the maximum deflections will be underestimated by about 35 percent *To obtain a good agreement of deflections, a value of* k *2.4 times lower should be used;* namely,

$$k = k_w = 0.42 \sqrt[3]{\frac{E_s}{E}} \frac{E_s}{(1 - \nu_s^2) h} \quad (10)$$

Similar conclusions can be reached by comparative study of solutions of the problem of a semi-infinite pavement slab loaded at its edge The solution of this problem by the subgrade reaction approach has been given by Westergaard (*34*), the solution by the elastic-solid approach has been found by Pickett, Badaruddin, and Ganguli (*35*). Comparisons of results can be made by using charts developed by Pickett and Ray (*13*) and Pickett and Badaruddin (*36*) It would be of interest to make similar comparisons for the corner case, although the contemporary trend in design of concrete pavements with doweled transverse joints makes this case less important from the practical point of view than it was in the past.

EFFECT OF LIMITED DEPTH OF COMPRESSIBLE SUBGRADE

All preceding considerations have been based on the assumption that the compressible subgrade under the pavement slab extends to an infinite depth However, in most real soil situations the compressible subgrade extends only to a finite depth, H, below which follows either a stratum of much lower compressibility or a stratum of rock, which for all practical purposes is incompressible. Thus, it is of particular interest to explore the effect of limited depth of compressible subgrade

With this purpose in mind, consider a slab of infinite extent and thickness h, resting on a subgrade consisting of an elastic-isotropic solid layer of finite thickness, H, overlying rock (Fig. 4). The rock layer is assumed to be infinitely stiff ($E_b = \infty$), whereas the solid above is characterized by a modulus of deformation, E_s, and a Poisson's ratio, ν_s. Under the action of a vertical point load, Q, the slab deflection at any point at a distance r from the load will be (*37*)

$$w = \frac{Q l_0^2}{D} \frac{H^2}{2\pi l_0^2} \int_0^\infty \frac{J_0 (\beta r/H)\, d\beta}{\beta^3 + (H/l_0)^3 \Phi(\beta)} = \frac{Q l_0^2}{D} I_w \quad (11)$$

in which l_0 is, as before, the stiffness radius, defined by Eq. 4, D is the flexural stiffness of the slab, defined by Eq. 5; J_0 is a Bessel function of zero order; β is a dimensionless parameter, and $\Phi(\beta)$ is a function defined by

$$\Phi(\beta) = \frac{\sinh \beta \cosh \beta + [\beta/(3 - 4\nu_s)]}{\sinh^2 \beta + [\beta/(3 - 4\nu_s)]^2} \quad (12)$$

With the same notations, the radial bending moment, M_r, is found to be

$$\frac{M}{Q} = \frac{H}{2\pi r} \int_0^\infty \frac{[\beta J_1 (\beta r/H) - (\beta^2 r/H) J_0 (\beta r/H)] d\beta}{\beta^3 + (H/l_0)^3 \Phi(\beta)} \quad (13)$$

The numerical values of the integrals in Eqs. 11 and 13 have been evaluated numerically for $\nu_s = 0.30$ by Hogg (*37*). The bending moments for a few characteristic depths of the compressible subgrade are shown in Figure 5 by solid lines; the dashed line shows the analogous moments as evaluated from the Hertz-Westergaard solution It is evident that the limited depth of the compressible subgrade has very little effect on bending moment and stresses in the slab as long as the depth of the subgrade stratum, H, exceeds about two stiffness radii of the slab. Even when the subgrade layer thickness is only one stiffness radius thick, the difference in bending moments and stresses is, for practical purposes, small.

It is not difficult to see that the effect of finite depth of the subgrade can be introduced into analysis through an increase in value of coefficient k, as determined by Eqs 8 or 9. For $H/l_0 = 2$ the apparent increase would be only 20 percent above the value given by Eq. 9; for $H/l_0 = 1$ the increase is still only about two-fold.

The values of deflections, as given by Eq. 11 in function of relative depth of compressible subgrade (expressed in stiffness radii), are plotted in Figure 6 as solid lines. Also shown (dashed line) is the deflection curve obtained by the Hertz-Westergaard solution under the assumption that the radius of relative stiffness is equal to l_0 as given by Eq. 4.

A closer study of Figure 6, in conjunction with Figure 5, reveals some interesting facts If the analysis of a slab resting on an elastic-isotropic solid of finite depth is made with the value of coefficient of subgrade reaction, k_0, suggested by Eq. 9, the agreement of deflections is improved as the thickness of the subgrade layer decreases. Thus, although the deflections obtained by using the mentioned k_0-value are underestimated by 35 percent when the subgrade has infinite thickness, they are underestimated by 20 percent if the subgrade is five stiffness radii thick, and only by 7 percent if the subgrade is three stiffness radii thick. When the subgrade becomes about 2½ radii thick, almost perfect agreement of both bending moments and deflections can be expected. As the thickness of the subgrade layer decreases further, this almost perfect agreement of both bending moments and deflections continues

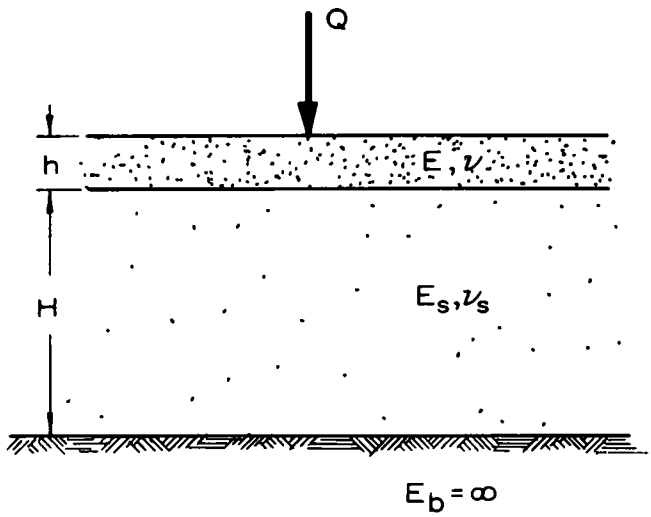

Figure 4 Infinite slab resting on an elastic solid of finite depth.

to exist, with a unique value of coefficient and subgrade reaction, k, which is generally higher than k_0.

A relatively brief analysis shows that this unique value of coefficient of subgrade reaction for an elastic-isotropic subgrade of finite thickness, H, can be given by

$$k_0' = 2.5\ (l_0/H)\ k_0 = \frac{1.38\ E_s}{(1-\nu_s^2)\ H} \qquad (14)$$

valid for $H/l_0 < 2.5$ or $H/h < 1.38 \sqrt[3]{E/E_s}$

It may be concluded that Winkler's hypothesis (*1*) is for

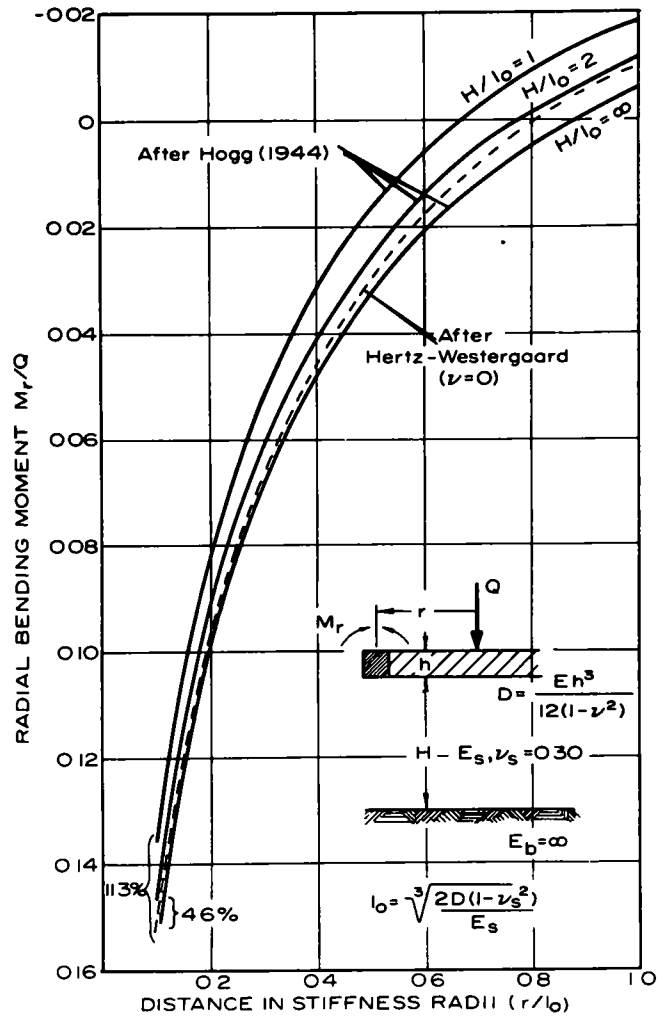

Figure 5. Bending moments in an infinite slab resting on an elastic solid of finite depth.

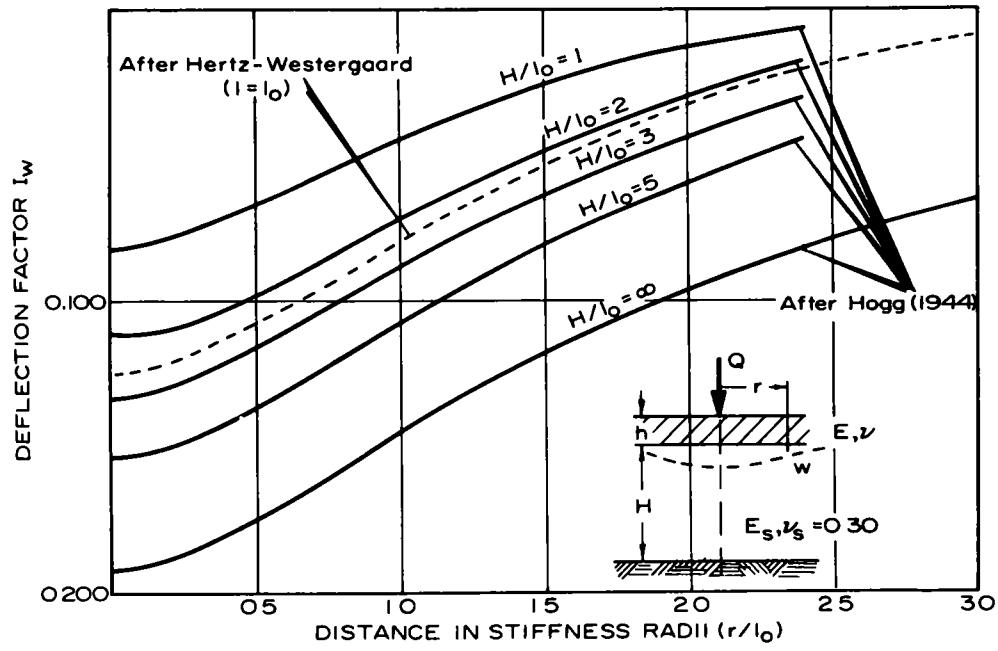

Figure 6. Deflection factors, I_w, for an infinite slab resting on an elastic solid of finite depth.

all practical purposes satisfied also for slabs resting on an elastic-isotropic solid subgrade of finite thickness, H, as long as this thickness does not exceed about 2 5 stiffness radii, l_0, defined by Eq. 4. The coefficient of subgrade reaction, k, of such slabs can be estimated by using Eq 14.

When the thickness of compressible subgrade exceeds about 2 5 stiffness radii, Winkler's hypothesis can still be used for analysis. However, the value of coefficient of subgrade reaction, $k = k_0$, that yields good agreement of pavement stresses will not provide good agreement of deflections as well. The deflection patterns will agree only if a lower value of $k = k_w$ is selected.

EVALUATION OF k FROM PLATE LOAD TESTS

It is of some interest to see how large circular rigid plate should indicate the same coefficient of subgrade reaction as that given by Eqs. 8 or 9 for a flexible slab. Computing $p/w = k$ from the well-known formula for deflection of a rigid circular plate of diameter B,

$$w = \frac{\pi p B(1 - \nu_s^2)}{4E_s} \tag{15}$$

the following plate diameter is found:

$$B = \frac{4}{\pi}\sqrt[3]{\frac{E}{E_s}}\, h \tag{16}$$

Knowing that typical E-values for concrete slabs may be around 5×10^6 psi and that E_s values for subgrades will most often be in the range of 5,000 to 50,000 psi, it may be concluded that the "representative" plate diameter that yields the proper value of coefficient k for concrete slabs would typically fall in the range between 6 and 12 slab thicknesses. A comparison with magnitudes of "range of influence" of slabs proposed by Terzaghi (*29*) reveals that the diameter given by Eq. 16 is about one-half of that recommended by Terzaghi.

It should be noted that Eq 15 is, strictly speaking, valid only for a subgrade of infinite depth and that the "settlement factor," $\pi/4$, becomes lower if the subgrade has a finite depth, H. For all practical purposes, however, the difference is small as long as H exceeds about $5B$ For smaller depths, H, there are charts and tables that give the appropriate value of the settlement factor (*38*).

CHAPTER TWO

DATA ON AASHO ROAD TEST RIGID PAVEMENTS

BASIC DATA ON PAVEMENT SECTIONS

As described in final reports on the AASHO Road Test (*39*), the main factorial experiment with rigid pavements consisted of accelerated load-testing of some 156 structural sections, of which 130 were of different design. Principal variables in these designs were the slab thicknesses and reinforcement, as well as subbase thicknesses. Basic data on all the structural sections are given in Table 3. Full details can be found in Table 12, *HRB Spec. Rep. 61A* (*39*)

The available data indicate that slab thicknesses varied between 2½ and 12½ in, and the subbase thicknesses between 0 and 9 in. All sections had lane widths of 12 ft. Sections that consisted of nonreinforced slabs had sawed, doweled transverse contraction joints spaced at 15 ft, thus forming 12 × 15-ft slab panels. Reinforced sections had sawed, doweled transverse contraction joints spaced at 40 ft, thus forming 12 × 40-ft slab panels. The reinforcement of these sections consisted of single welded wire fabric, placed 1¼ to 2 in. deep in the pavement slabs. The weight of the fabric was consistent with pavement thickness, representing, in each direction, approximately 0.1 percent of the cross-sectional area of the pavement. The size of dowels in transverse joints was increasing according to the slab thickness from ⅜ in. in diameter and 12 in. in length to 1⅝ in. in diameter and 18 in. in length. Longitudinal joints were reinforced with tie-bars, increasing in size with slab thickness from No. 3, 20 in long, to No. 5, 30 in long Details about joints, reinforcement, dowels, and tie-bars can be found in Table 7, *HRB Spec Rep. 61A* (*39*).

STRUCTURAL BEHAVIOR

Principal quantitative information on structural behavior of the AASHO Road Test rigid pavements can be obtained from the measurements of pavement strains and deflections under load. Such measurements were made in the main traffic loops (2 through 6) as a part of routine load testing by moving trucks.

Strains were measured by electrical strain gauges placed in the middle of slab panels (for 15-ft-long nonreinforced sections) or at 10 ft from the joints in each panel (for 40-ft-long reinforced sections). All these gauges were placed parallel to the slab edges at a distance of 1 in. from the

TABLE 3

RIGID PAVEMENT SECTIONS OF THE AASHO TEST ROAD[a]

LOOP	AXLE LOAD[b] (KIPS) LANE 1	LANE 2	SLAE THICKNESS (IN)	SUBBASE THICKNESS (IN.)
1	None	None	2½, 5, 9½ and 12½	0 and 6
2	2–S	6–S	2½, 3½ and 5	0,3 and 6
3	12–S	24–T	3½, 5, 6½ and 8	3,6 and 9
4	18–S	32–T	5, 6½, 8 and 9½	3,6 and 9
5	22 4–S	40–T	6½, 8, 9½ and 11	3,6 and 9
6	30–S	48–T	8, 9½, 11 and 12½	3,6 and 9

[a] All sections in both plain and reinforced concrete
[b] S=single, T=tandem

edges Deflections under moving loads were measured by electrical deflectometers (LVDT) placed in pairs at slab edges 6 in. from transverse joints. Rebound deflections under static loads were measured by means of a Benkelman beam. Details about these measurements can be found in *HRB Spec Rep 61E* (*39*), in particular Art. 3.3.1, Tables 56 and 57, and Figures 138 through 147, as well as in a paper presented at the St Louis Conference by Hudson and Scrivner (*40*).

In addition to mentioned strain and deflection measurements under moving truck loads, a special experimental study of strains across pavement slabs under the action of an oscillating load simulating a single wheel loading was performed in Loop 1, which otherwise was not subjected to any truck loads For the purpose of this study 6 × 6-ft square corner areas of slab sections were equipped with electrical strain gauges. These gauges were placed either singly (along the slab edges and along the transverse joint edges), or grouped in rosettes of three gauges (for measuring points inside the pavement slab panels). The exact layout of these strain gauges is detailed in Figure 170, *HRB Spec. Rep. 61E* (*39*).

The loads were transmitted to the pavement through two 11 × 14-in. wooden pads spaced 6 ft, center to center, in 14 different positions. The loads were varied sinusoidally with time at a frequency of 6 cycles per second, from a minimum of 500 lb to a maximum that varied from 12,000 lb for the 5-in.-thick slab to 30,000 lb for the 12.5-in.-thick slab. All essential details about these special tests are given in Art 3 5.4, *HRB Spec. Rep. 61E* (*39*), as well as by Hudson and Scrivner (*40*).

Special deflection measurements were performed by the Ohio River Division Laboratories, Corps of Engineers, U.S. Army (*41*). In this investigation the entire deflection basins around loaded areas on AASHO rigid pavement sections were measured, thus offering most valuable quantitative information about the response of pavement slabs to loads.

Important information on structural behavior of AASHO Road Test rigid pavements was also collected by considering the modes of failure of different pavement slabs. Such information is not purely qualitative, because the crack pattern may be indicative of the location of points in the pavement slab panels where the stresses are the highest. The principal information on crack patterns observed can be found in Art. 3.2.3, *HRB Spec. Rep. 61E* (*39*), as well as in a paper presented at the St. Louis Conference by Scrivner (*42*).

MECHANICAL PROPERTIES OF PAVEMENT MATERIALS AND SUBGRADE

For analysis of structural behavior of the AASHO Road Test pavement system it is essential to have a thorough knowledge of the mechanical properties of the materials of the system, including the subgrade. Of particular significance are those properties which characterize the response of the pavement material to loads Because no testing was included in the research program of the present investigation, the evaluation of the material properties is based on existing published data from other investigations connected with the AASHO Road Test.

Concrete Slabs

The concrete for pavement slabs was made of Type I portland cement, water, air-entraining agent, fine aggregate, and a coarse aggregate whose maximum size was either 2½ or 1½ in., depending on slab thickness. Details about properties of individual components of this material and construction procedures used can be found in *HRB Spec. Rep. 61B* (*39*), Chapter 6. The principal mechanical properties of this material, as determined by standard AASHO tests on 6 × 12-in. cylinders, or 6 × 6 × 30-in. beams, are given in Table 4.

Subbase

The subbase material for the rigid pavement systems was made of a sand-gravel mixture, stabilized with a friable fine-grained soil and compacted according to AASHO specifications. Details about properties of components of this material and the construction procedures used can be found in *HRB Spec. Rep. 61B* (*39*), Chapter 3. Principal characteristics of this material are summarized in Table 5.

TABLE 4

MECHANICAL PROPERTIES OF AASHO ROAD TEST CONCRETE SLABS

SLABS			COMP. STRENGTH (LB/IN.^{2})		FLEX. STRENGTH (LB/IN.^{2})	
TYPE	THICKNESS, h (IN.)	MAX. AGGR SIZE (IN.)	21 DAYS	1 YEAR	21 DAYS	1 YEAR
Thicker	≥ 5.0	2.5	4,130	5,580	660	790
Thinner	2.5 and 3.5	1.5	4,250	5,990	710	880

Subgrade

The subgrade was constructed by compacting a locally available yellow-brown silty clay (A-6 material in the BPR classification). Principal index properties of this soil are summarized in Table 6. More details can be found in *HRB Spec. Rep. 61B* (*39*), Chapter 2.

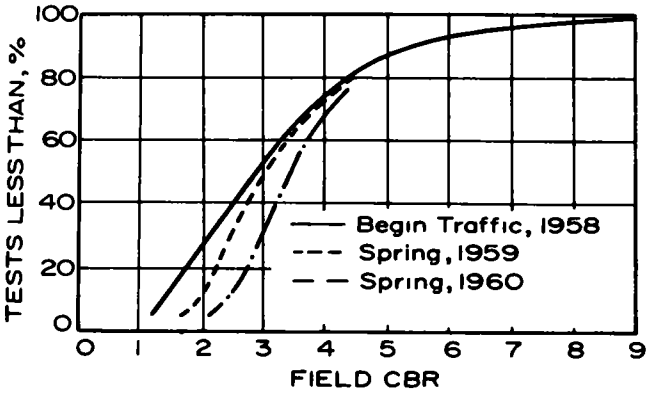

Figure 7. Field CBR values of the AASHO subgrade soil (after Finn, Ref. 44).

TABLE 5

PHYSICAL CHARACTERISTICS OF SUBBASE MATERIAL

Textural classification:	Sand-gravel mulch	
Grain-size distribution:	*Sieve No. or Grain Size*	*Percent Finer Than*
	1 in.	100
	¾ in.	96
	½ in.	90
	No. 4	71
	No. 10	52
	No. 40	25
	No. 200	6.5

Atterberg limits: Non-plastic
Specific gravity: 2.70
Compacted density: 134.5 lb/cu ft
Corresponding moisture content: 3.8 percent
Mean CBR value: 34.7

Of particular interest to this investigation are the deformation characteristics of this subgrade—its modulus of deformation, E, and its Poisson's ratio. A review of experimental data available on these two characteristics for the AASHO Road Test, made several years ago in connection with a study of structural behavior of AASHO flexible pavements (*43*), disclosed a wide variation of modulus of deformation measured by different organizations engaged in testing of the AASHO subgrade. In addition to variation of E-values attributed to the difference in testing methods used by different organizations, there was also significant variation of results within one investigation, reflecting the sensitivity of deformation characteristics to variations in moisture content, soil density, stress level, and number of stress repetitions. A summary of measured values of E is presented in Table 7.

Perhaps the most instructive information on variation of deformation characteristics of the AASHO subgrade in field conditions can be found in distribution curves of field CBR values of that soil presented in discussion at the St. Louis Conference by Finn (*44*), and reproduced herein as Figure 7. These distribution curves indicate that the actual

TABLE 6

PHYSICAL CHARACTERISTICS OF SUBGRADE MATERIAL

Textural classification:	Yellow-brown silty clay (A-6)	
Grain-size distribution:	*Sieve No. or Grain Size*	*Percent Finer Than*
	No. 4	99.0
	No. 10	96.8
	No. 40	91.0
	No. 60	87.7
	No. 200	80.6
	0.02 mm	62.8
	0.05 mm	42.3
	0.002 mm	15.3

Atterberg limits: Liquid limit = 29.4 percent
Plastic limit = 16.5 percent
Specific gravity: 2.71
Compacted density: 115.4 lb/cu ft
Corresponding moisture content: 15.5 percent
Maximum density: 116.4 lb/cu ft
Optimum moisture content: 15.1 percent
Mean CBR value: At time of paving = 1.7
Under traffic = 3.0

TABLE 7

MODULUS OF DEFORMATION OF AASHO ROAD TEST SUBGRADE

INVESTIGATING AGENCY	BASIS FOR DETERMINATION	MODULUS OF DEFORMATION, E, (LB/IN^2)	REF.
Kansas Highway Dept	Triaxial compression test	1,300[a]	(*45*)
Univ. of California	Triaxial compression test	5,500	(*46*)
Asphalt Institute	Van der Poels stiffness factor	3,000	(*52*)
Ohio State Univ	Triaxial compression tests	4,000	(*47*)
Georgia Inst. Tech	Triaxial compression tests	1,040[a]	(*48*)
Indirect determination	From plate load tests	2,040	(*43*)
	From CBR tests	2,800–5,600	(*43*)
	From measured pavement deflections	7,000	(*43*)

[a] Initial tangent modulus

deformation moduli of the AASHO Road Test subgrade varied within the limits of 50 percent to 200 percent of the average values measured. They also indicate that some increase of deformation moduli of the subgrade may have occurred as the Road Test progressed. The indicated variations of deformation characteristics of the subgrade have been taken into account in the subsequent analysis (Chapter Three).

CHAPTER THREE

ANALYSIS OF TEST RESULTS AND FINDINGS

Previous analyses of strain measurements made on the AASHO Road Test rigid pavements (*40*) have brought to light several important features of structural behavior of these pavements. It was found, for example, that for a given pavement at a given time the strains varied linearly with load and that the subbase thickness and the degree of slab reinforcing did not have systematic effects on observed strains. Comparisons between strains measured in Loop 1 tests, using stationary oscillating loads transmitted through wooden pads, and strains measured in other loops under moving truck loads showed essentially the same strains under comparable loads. A direct correlation was established between strains measured along the pavement edges under moving loads and pavement performance. Such a correlation confirms the basic philosophy of existing rigid pavement design methods, which are mostly based on considerations of maximum tensile stress in the pavement slabs. However, no attempt was made to compare the measured strains, which can be converted into stresses, with theoretical predictions.

To make comparisons of this kind, it is essential to possess a method of evaluation of deformation characteristics of the subgrade, most often represented by coefficients of subgrade reaction, as well as to possess a method of quick analysis of any pavement slab with arbitrary end conditions and under arbitrary loading. The developments in Chapter One make it possible, for the first time, to predict reliably the coefficients of subgrade reaction of the slab/subgrade systems used in the AASHO Road Test on the basis of mechanical properties of the slabs and the AASHO subgrade, reported in Chapter Two. At the same time, recent developments in finite element methods of analysis of slabs and in computer science have made it possible to prepare a computer program for analysis of any pavement slab situation. The details of this program, which is based on a finite element model first proposed by Newmark (*49*) and extensively developed by Hudson and Matlock (*50, 51*) are given in Appendix A.

DETERMINATION OF AVERAGE VALUE OF k FOR THE SUBGRADE

The values of the coefficient of subgrade reaction, k, for the AASHO subgrade have been determined in previous studies of AASHO Road Test results primarily by two established methods. One of these is the method developed by the

Bureau of Public Roads following the Arlington tests (*7*), which defines k as the ratio of unit pressure and rebound deflection of a 30-in -diameter rigid plate Field tests under rigid pavement sections of the AASHO Road Test in the spring of 1960 using this method yielded average k-values of 86 lb/in ^{3} for tests on subgrade alone and 108 lb/in.^{3} for tests on subbase. The second method, developed and used by the Ohio River Division Laboratory of the Corps of Engineers (*41*) is based on measurements of entire deflection basins of loaded pavement slabs. According to this method the coefficient k is defined as the ratio of applied load and the volume of deflection basin of the loaded slab. Measurements by the Ohio River Division Laboratories staff, made in 1961, on 16 rigid pavement sections of Loops 2 and 3, yielded k-values varying from 25.9 to 92.2 lb/in ^{3}

It is significant to note that the k-values determined by the latter method show definitely a trend suggested by Eq 9; namely, that the coefficient k depends on slab thickness, as well as on the deformation characteristics of the subgrade. Although there is appreciable scattering of individual test values, the average value of k measured from 17 through 29 May, 1961, on 5-in. slabs is 46 5 lb/in ^{3}, the average k for 3 5-in slabs for the same period is 70 0 lb/in.^{3} These two values are almost exactly in inverse proportion to slab thickness, as suggested by Eq 9

For proper determination of k by using Eq. 9 it is essential to know the modulus of deformation of the subgrade, E_s As mentioned in Chapter Two, this modulus may vary rather sharply with the moisture content and density of the subgrade soil. As mentioned earlier, the best indication of the range of variation of this parameter in actual field conditions of the AASHO Road Test can be assessed from studies of variation of field CBR values of the subgrade, the results of which are shown in Figure 7. The CBR values in the field varied from about 1 5 to more than 7, which, in terms of E_s-values may be interpreted to mean variations from about 2,100 lb/in ^{2} to more than 10,800 lb/in.^{2} Assuming, for May-June 1961, an average value of CBR = 3.6 or $E_s = 5{,}400$ lb/in.^{2} with $\nu_s = 0.33$ and with concrete characteristics from Table 3, one obtains for the 3 5-in -thick slab a coefficient k_0 of 165.4 lb/in.^{3} and for the 5 0-in -thick slab $k_0 = 115\ 6$ lb/in ^{3} According to theory discussed in Chapter One, to obtain good agreement of pavement slab deflections one should select a k-value equal to 0.42 k_0 This gives for the 3 5-in slab a k-value of 69 5 lb/in ^{3} and for the 5 0-in slab a k-value of 48 5 Considering the uncertainties in selection of representative CBR value for the period of testing, as well as uncertainties of the conversion of CBR into E_s-values, the agreement of these values with actually observed ones (70 0 and 46 5) should be considered remarkable

To find a proper value of k for analysis of strain measurements in Loop 1, as well as in traffic Loops 2 through 6, a representative average value of CBR = 3 has been selected This furnishes an E_s-value of 4,500 lb/in.^{2} and the k_0-values for different slabs given in Table 8. These values have been used in the analyses of strain data presented in the following sections.

TABLE 8

VALUES OF COEFFICIENT OF SUBGRADE REACTION, k_o, FOR PAVEMENT SLABS OF THE AASHO ROAD TEST

SLAB THICKNESS, h (IN)	COEFFICIENT OF SUBGRADE REACTION,[a] k_o (LB/IN ^{3})
2 5	180 8
3 5	129 0
5 0	90 4
6 5	69 5
8 0	56 5
9 5	47 5
11 0	41 1
12 5	36 2

[a] k_o after Eq 8, with E_s=4,500 lb/in ^{2}, ν_s=0 33, E- and ν-values from Table 4

STRAIN MEASUREMENTS IN LOOP 1

As mentioned earlier, complete measurements of strains under oscillating loads (simulating a typical single-wheel, dual-tire assembly) have been made on several slab panels of Loop 1. From measurements made in strain rosettes, principal strains were computed and subsequently converted into principal stresses using the deformation characteristics of concrete as determined by laboratory tests (Table 4). The stresses so determined were used to plot contours of principal stresses, reproduced in Figures 187 through 190 of *HRB Spec Rep 61E* (*39*)

A complete structural analysis of the 12 loading cases represented in these figures was made using the computer program developed in the investigation reported here (see Appendix A), as well as the coefficient of subgrade reaction values presented in Table 8. The computed stresses along two characteristic sections for each loaded slab case are shown in Figures 8 through 19 (solid lines). The (a) part of these figures shows extreme fiber stresses, σ_y, along the free edge of the slab (acting in the longitudinal direction, y, of the slab). The (b) part of these figures shows extreme fiber stresses, σ_x, along a transverse axis connecting the centers of loaded areas (acting in transverse direction, x, of the slab). Also shown in these figures (black dots) are corresponding stresses evaluated (with deformation characteristics of concrete from Table 4) from surface strains measured in conditions where slab ends were warped upward

A study of these figures reveals very good to excellent agreement of computed and measured stresses, at least when the loads are applied at some distance from the doweled transverse joints. For load positions closer to these joints there was a tendency of measured stresses to be higher than those computed This is shown in Figure 20, which presents a comparison between computed and observed maximum edge stresses, σ_y, in function of distance of the simulated single wheel load from the doweled joint. A study of this figure, along with other available data, reveals that the differences between computed and observed

stresses can be explained by imperfect action of the doweled joints It is significant, for example, that the stresses in load position 2 (loads 2 ft from the joint) are almost as high as those in load positions 3 and 4 (loads 4 and 6 ft from the joint, respectively), although the computations show that the joint effect should have resulted in substantial reduction of these stresses. The imperfect action of the joint is, for obvious reasons, more pronounced in the thicker (12.5-in.) slab than in the thin (5-in.) slab.

STRAIN MEASUREMENTS IN MAIN LOOPS

Strain measurements in main loops were made on single strain gauges placed in the middle of 12 × 15-ft slab panels at a distance 1 in. from the pavement edge. According to *HRB Spec Rep 61E* (*39*), these measurements were made with the center of outer wheels positioned between 17 and 22 in from the pavement edge The average strains so measured, converted into stresses by using the *E*-value for concrete given in Table 4, are given in Table 9. Also given in this table are theoretical stresses at the pavement edge in the middle of the slab panels computed by using *k*-values from Table 8 and considering the outer wheel load at 18 in. from the pavement edge. The measured and computed stresses are also compared in Figure 21.

It is evident that the measured stresses are generally higher than the computed ones However, considering the fact that the stresses were measured at 1 in. from the pavement edge, which according to some limited computations should give about 10 percent higher stresses, it may be stated that there exists a reasonable agreement of computed and observed stresses for tandem-axle loads, with the exception of 3.5-in. slab measurements.

It is noted that, generally, there is more discrepancy between measured and observed stresses for thinner slabs. Probable explanation for this lies in greater susceptibility of these slabs toward partial loss of subgrade support due to slab warping.

It is also noted that the stresses in thinner slabs are much more sensitive to variations in transverse position of the wheels. This is shown in Figure 22, which shows edge stress in the middle of a slab panel as a function of distance of the outer wheel from the pavement edge. It appears that the ratio of measured and computed stresses increases in some proportion to the slope of the curves in Figure 22. However, at this stage and with the data now available it is hard to judge whether this observation is of any significance. To explain some of the high stress values observed, the loads would need to be moved up to 8 in. toward the pavement edge. The load placement data indicate that in normal test conditions such deviation was quite common, the whole range of load distances being more than ±2 ft from the programmed placement position. Yet the reports available (*39*) are firm in stating that all truck passes at improper distances from the pavement edge were excluded from consideration. Relying on this, it appears more plausible to accept the first explanation, in spite of the fact that this explanation cannot account for exceptionally good agreement of tandex-axle stress measurements.

TABLE 9

COMPARISON OF MEASURED AND COMPUTED MAIN-LOOP STRESSES

AXLE LOAD,[a] Q (KIPS)	SLAB THICKNESS, h (IN.)	EDGE STRESS, σ_y (LB/IN.^{2})		RATIO, MEAS
		MEASURED	COMPUTED	COMP.
6S	2 5	259	128	2.02
12S	3 5	337	214	1 57
	5 0	214	154	1 39
	6 5	153	118	1 30
18S	5 0	321	231	1.39
	6 5	229	177	1.30
22 4S	6 5	285	220	1 30
	8 0	219	178	1 23
30S	8 0	293	238	1.23
	9 5	235	182	1 29
24T	5 0	158	139	1 13
	6 5	126	114	1.10
32T	5 0	210	186	1 13
	6 5	168	152	1 10
	8 0	141	134	1 05
40T	6 5	210	190	1 10
	8 0	176	168	1 05
	9 5	152	126	1 20
48T	8 0	211	201	1 05
	9 5	182	151	1 20
	11 0	161	138	1 16

[a] S=single, T=tandem

DEFLECTION MEASUREMENTS IN MAIN LOOPS

As mentioned earlier, deflections were measured under moving loads by electrical deflectometers (LVDT) placed in pairs at slab edges 6 in. from transverse joints. Rebound deflections under static loads were measured by means of a Benkelman beam, using the general arrangement shown in Figure 145 of *HRB Spec. Rep. 61E* (*39*). A few typical results of these measurements are presented in Table 10, together with deflections computed by using Hertz-Westergaard theory and *k*-values given in Table 8.

A comparison of measured and computed deflections reveals first that all computed deflections are at least twice as large as the measured deflections. The differences are greater for corner deflections, and thicker slabs, suggesting definitely imperfect action of the joints, apparent already from strain measurements in Loop 1.

This finding is not in general agreement with theoretical predictions presented in Chapter Two and appears also to contradict the strain measurements in the main loops. A possible explanation for this apparent discrepancy may be sought in the differences in pressure distribution close to the edges of slabs resting on an elastic solid, as compared to slabs resting on a Winkler subgrade. However, considering the position of "fixed points" against which the deflections measurements were taken and the actual size of deflection basins of loaded pavement slabs, the possibility of experimental error of the order of magnitude in question (0.03 in.) should not be entirely excluded.

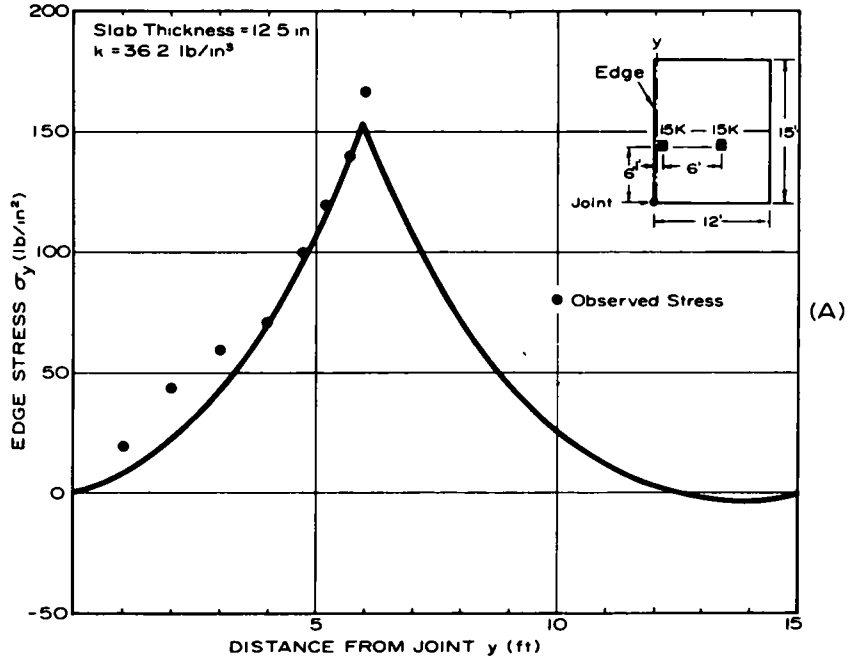

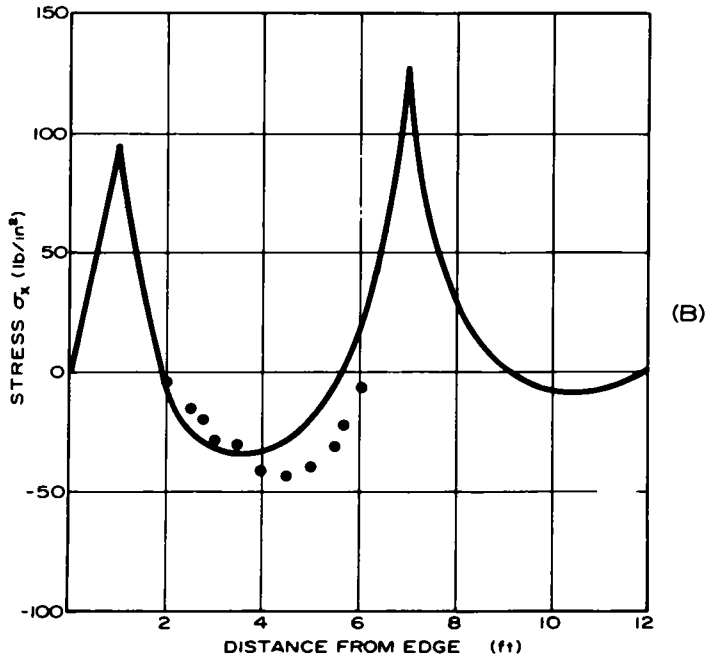

Figure 8. Stresses in 12 5-in. slab caused by 30-kip single-axle load 6 ft from joint, Loop 1.

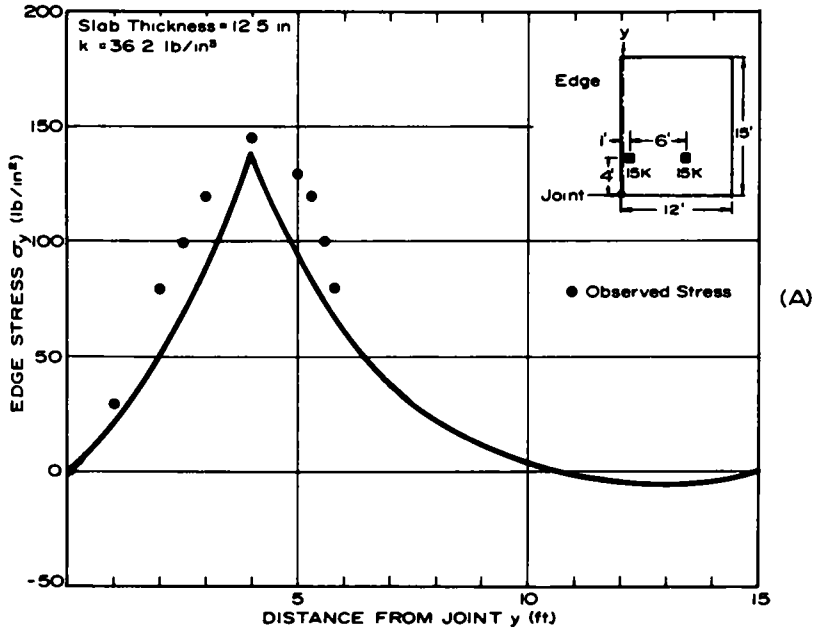

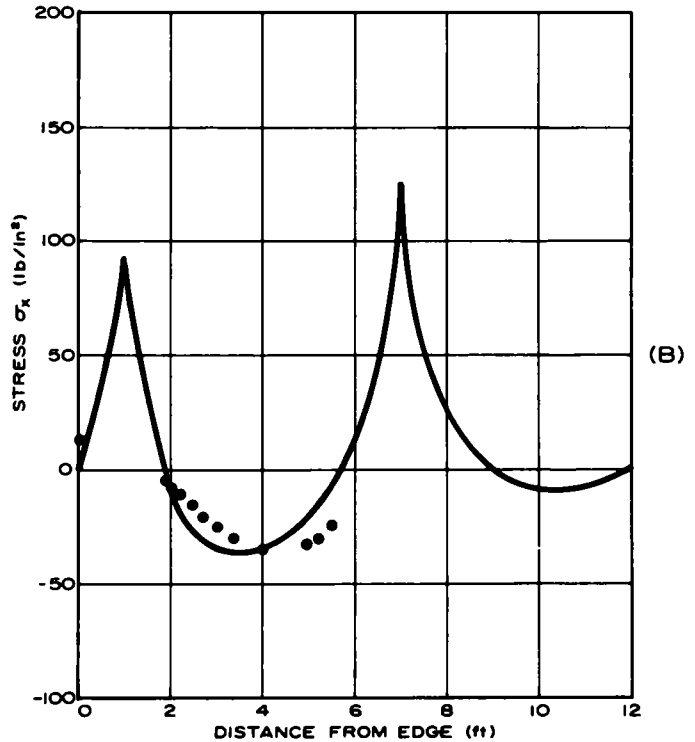

Figure 9 Stresses in 12 5-in slab caused by 30-kip single-axle load 4 ft from joint, Loop 1.

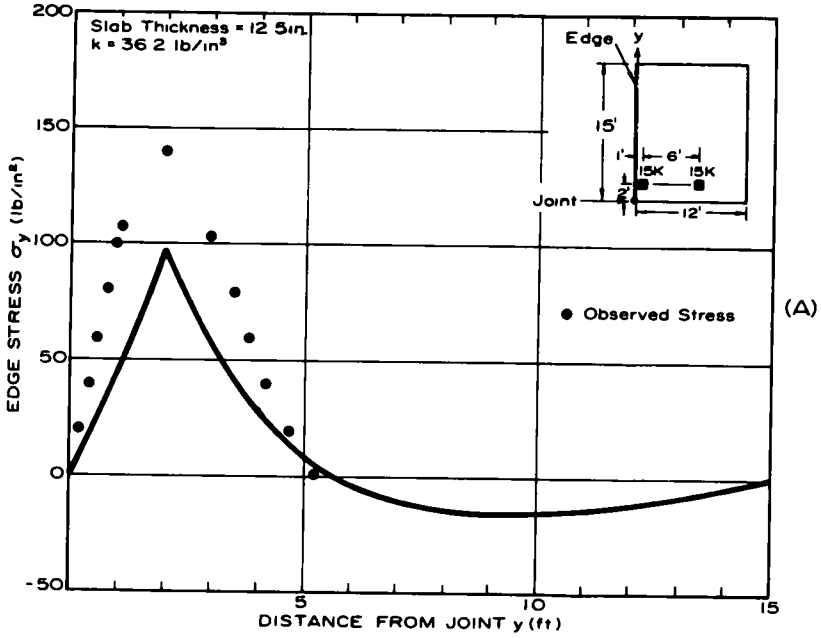

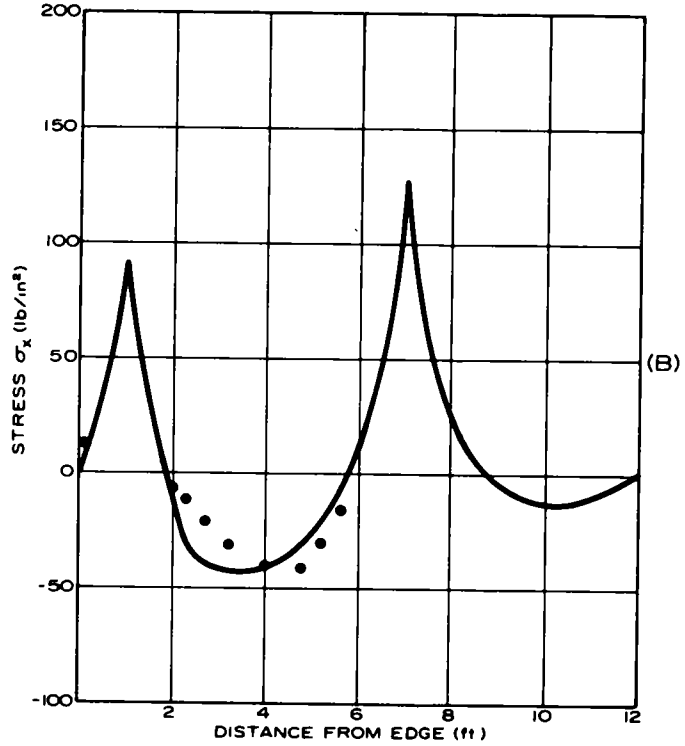

Figure 10. Stresses in 12 5-in. slab caused by 30-kip single-axle load 2 ft from joint; Loop 1.

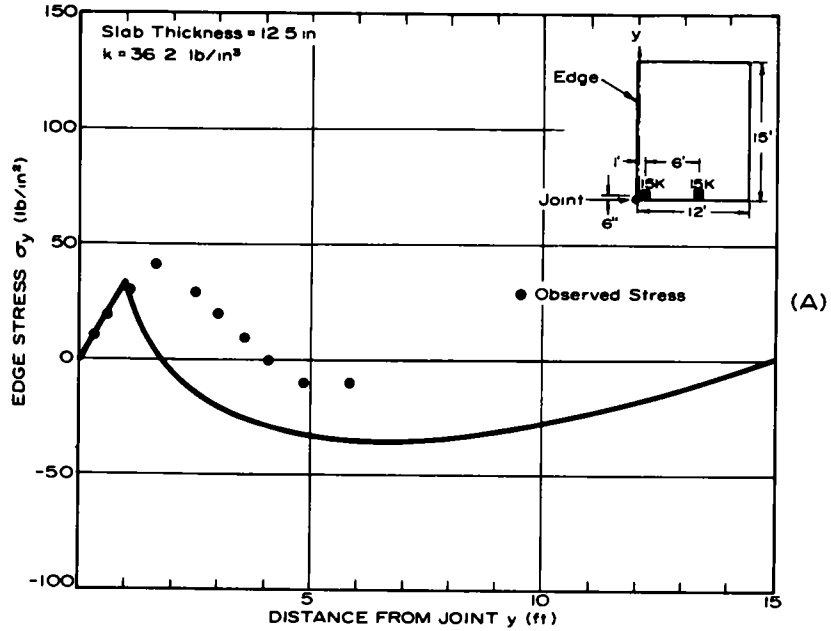

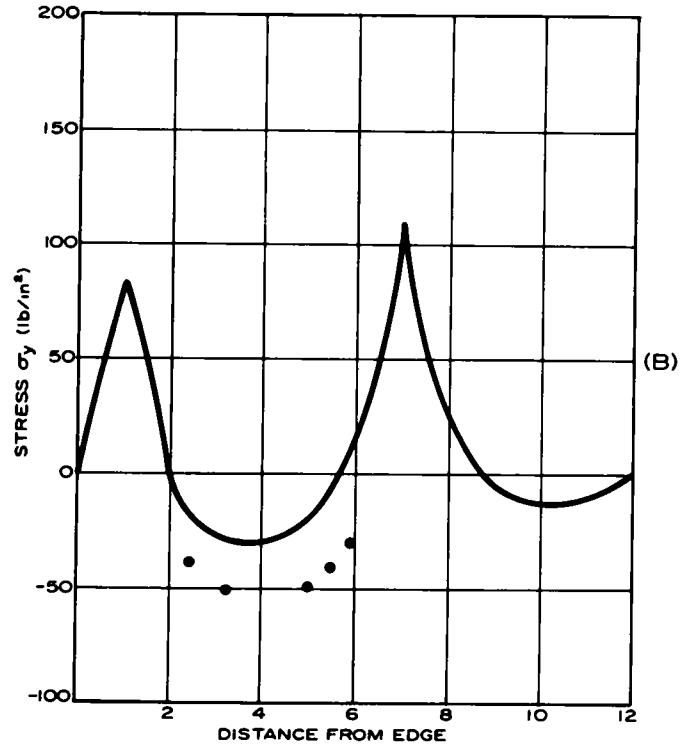

Figure 11 Stresses in 12 5-in. slab caused by 30-kip single-axle load 6 in. from joint; Loop 1

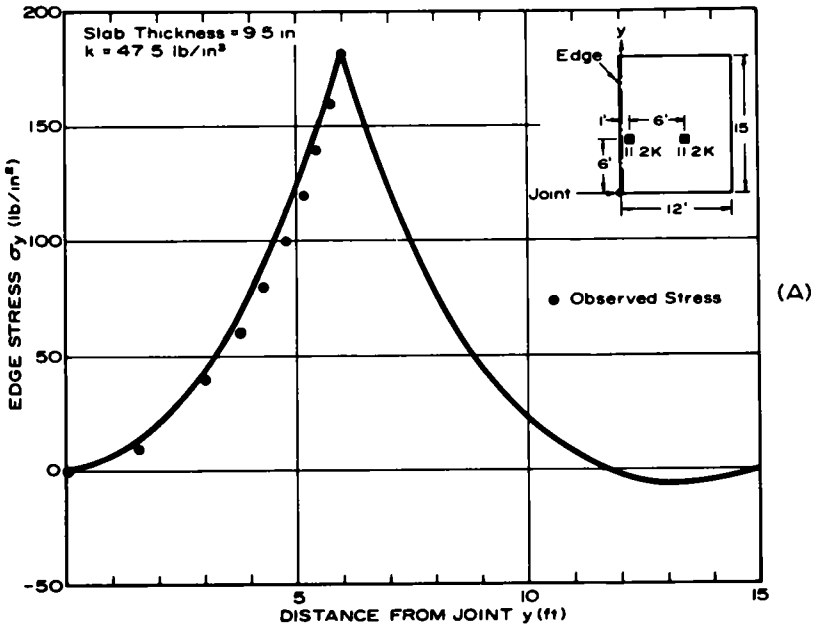

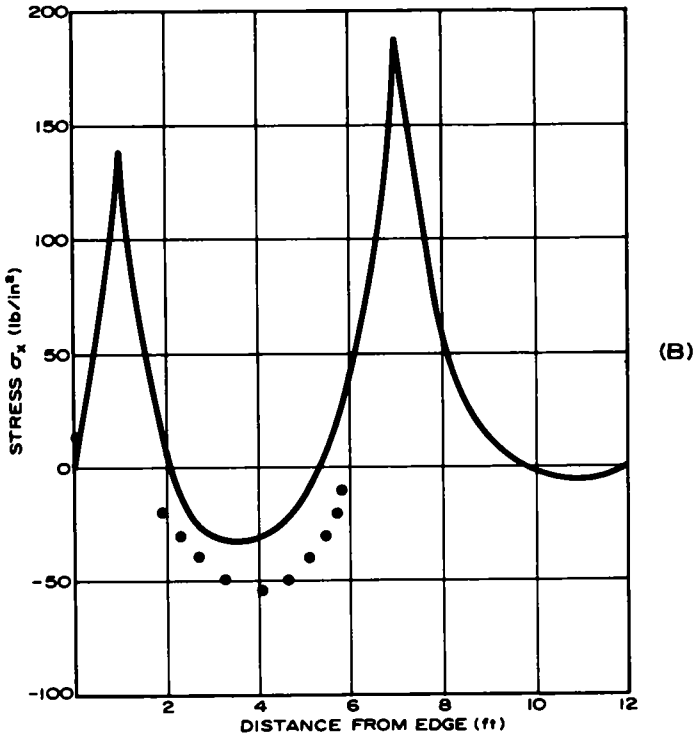

Figure 12. Stresses in 9 5-in. slab caused by 22.4-kip single-axle load 6 ft from joint, Loop 1

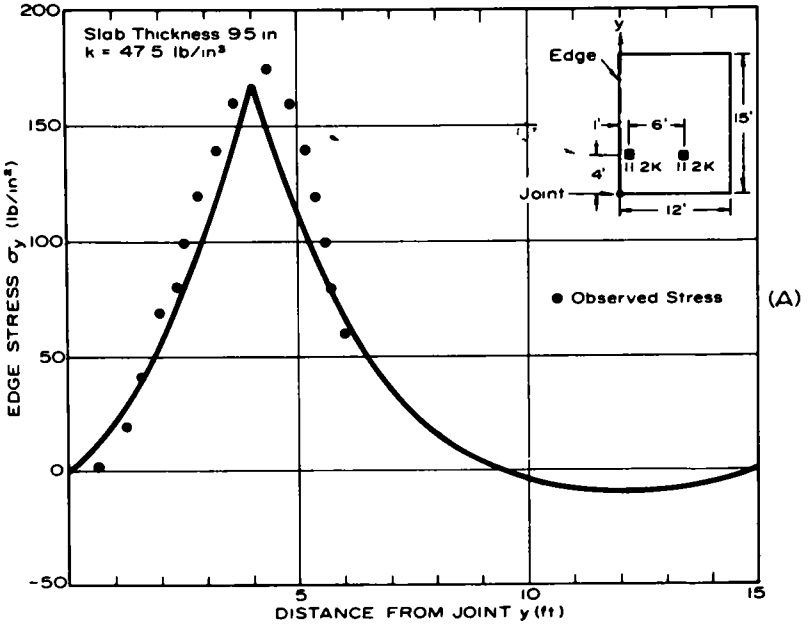

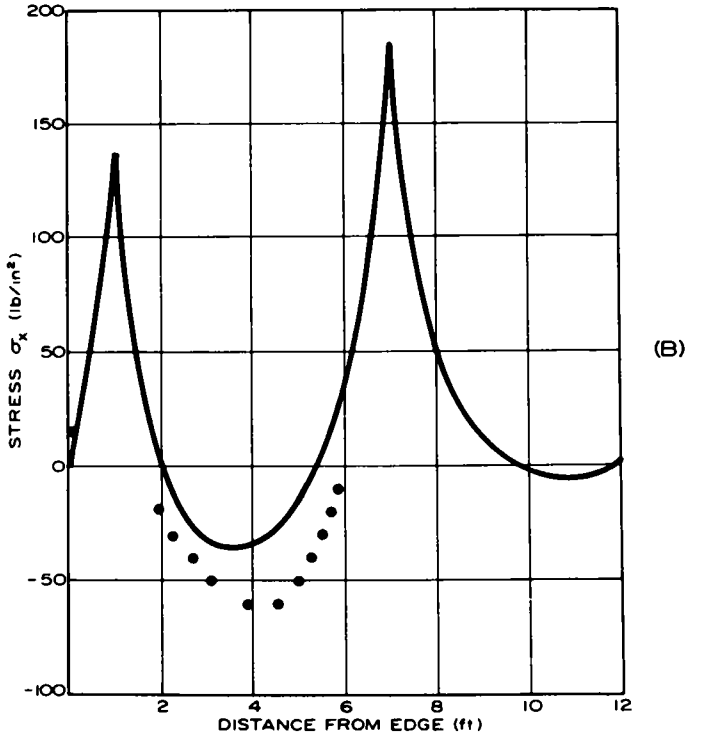

Figure 13. Stresses in 9 5-in slab caused by 22.4-kip single-axle load 4 ft from joint, Loop 1

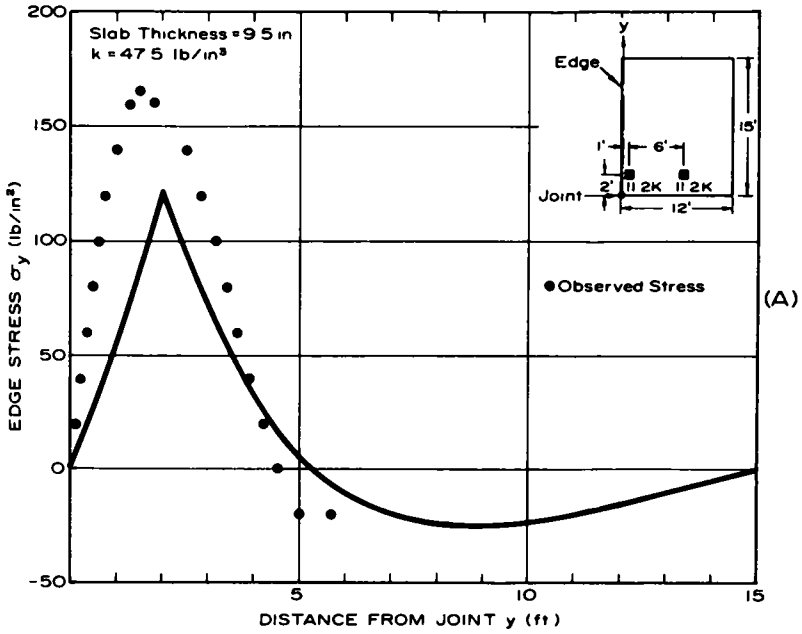

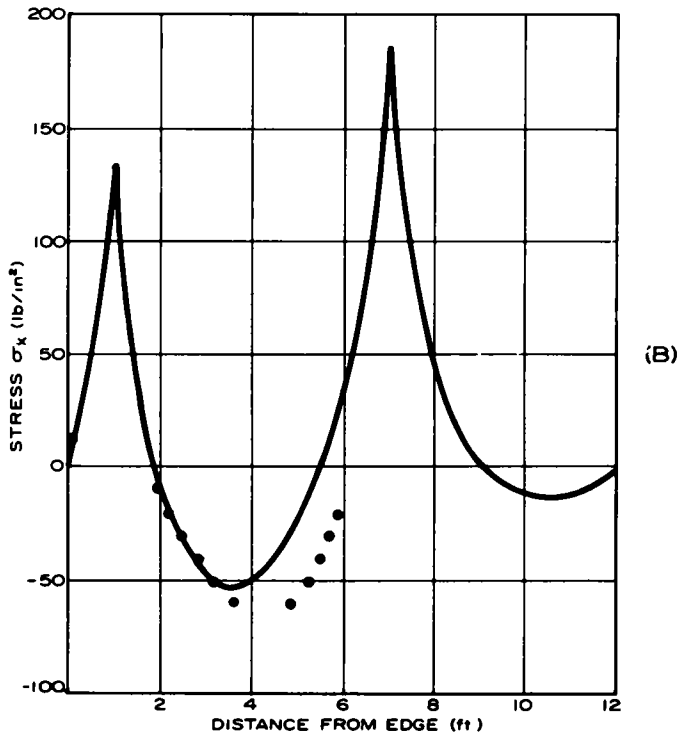

Figure 14 Stresses in 9.5-in. slab caused by 22 4-kip single-axle load 2 ft from joint; Loop 1

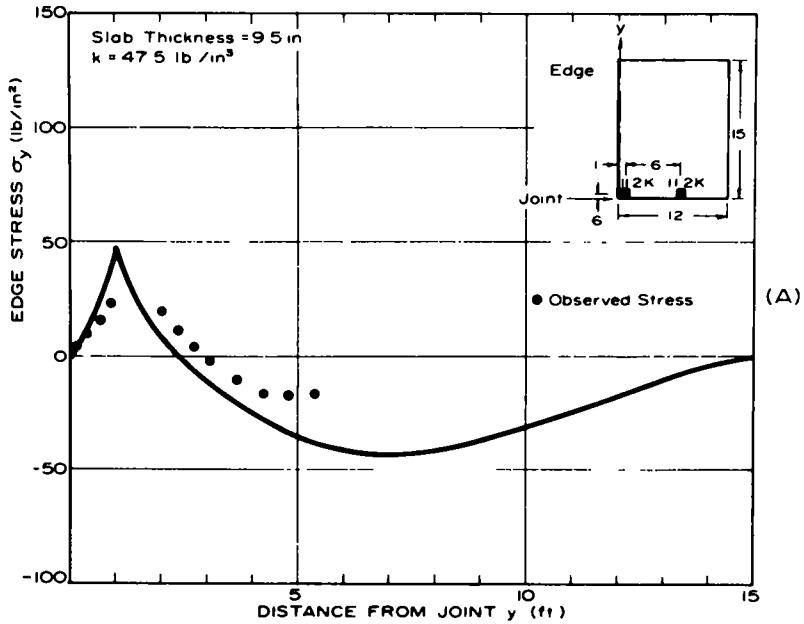

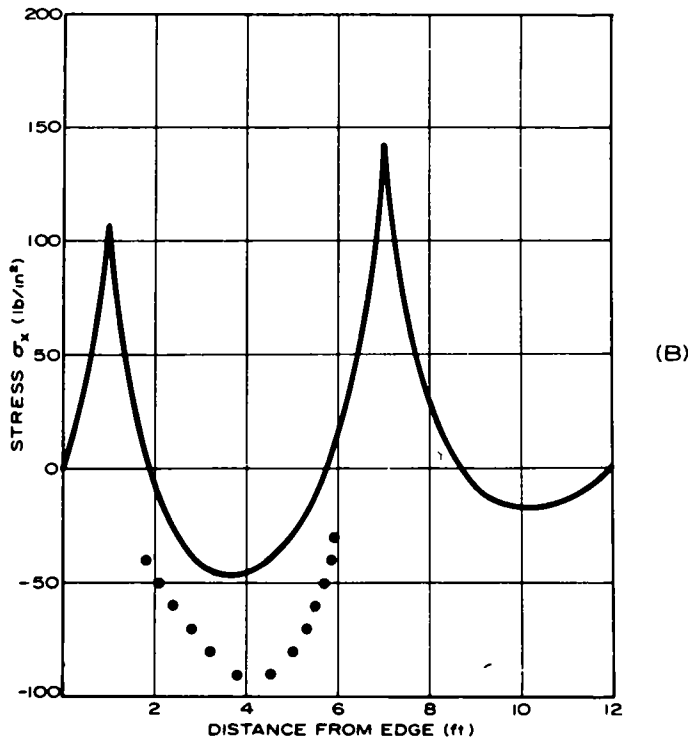

Figure 15. Stresses in 9 5-in slab caused by 22.4-kip single-axle load 6 in. from joint; Loop 1.

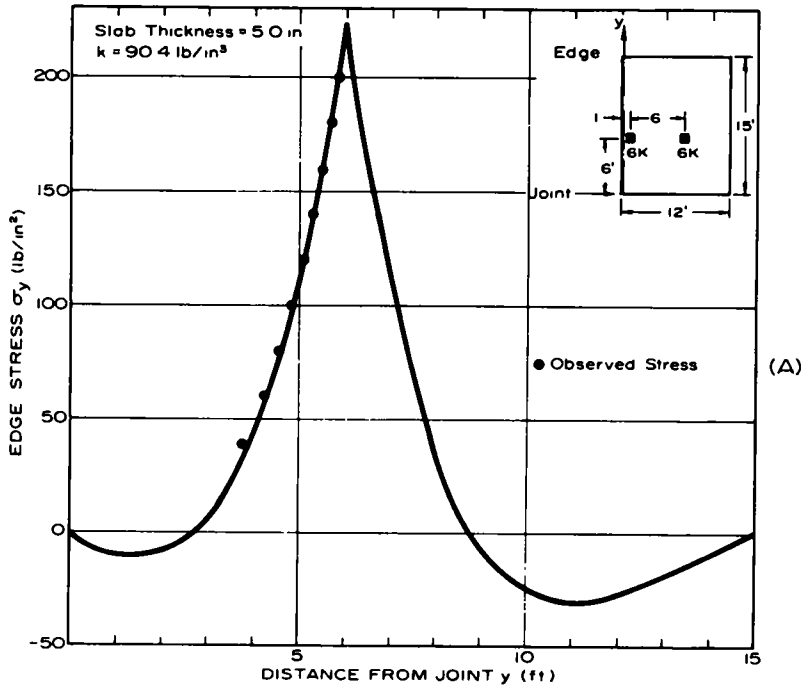

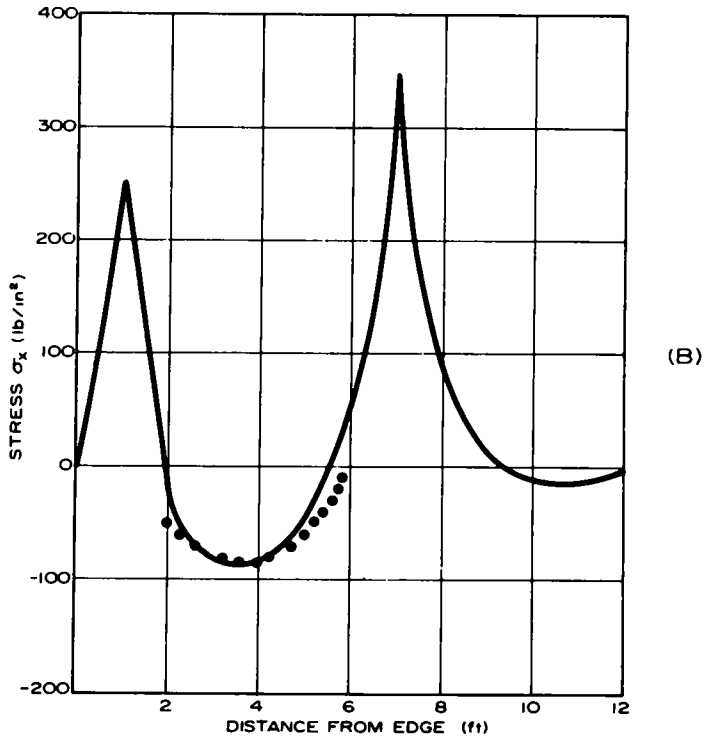

Figure 16 Stresses in 5.0-in. slab caused by 12-kip single-axle load 6 ft from joint. Loop 1.

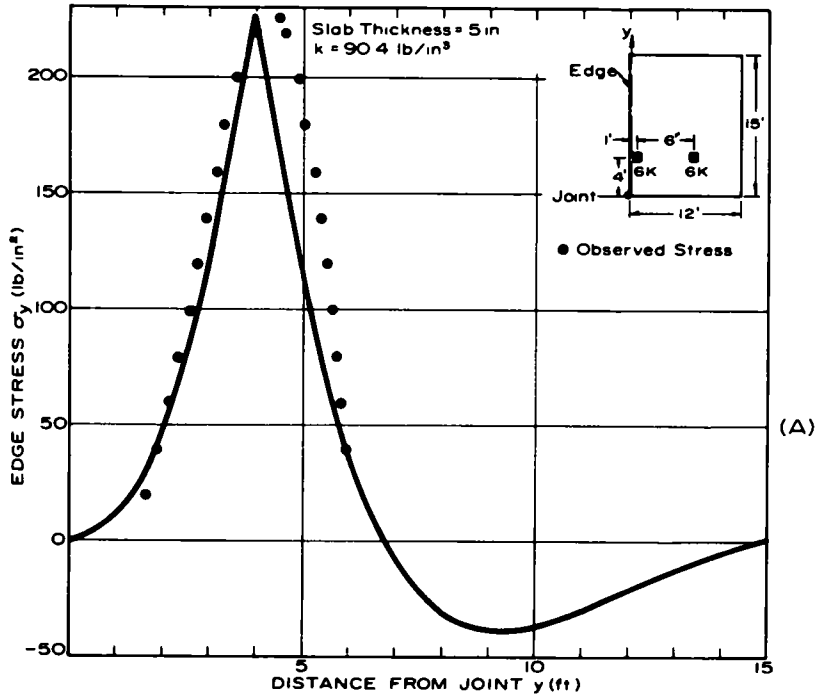

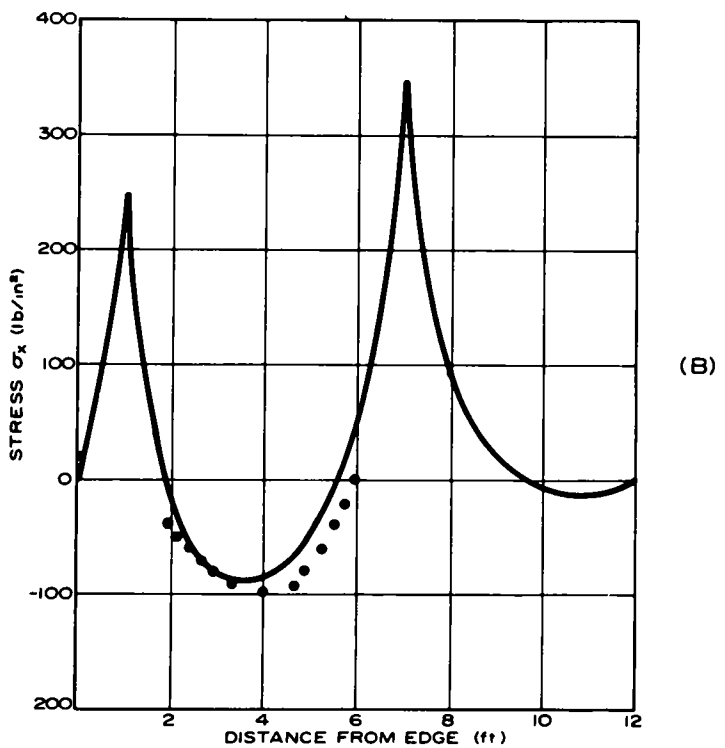

Figure 17. Stresses in 5.0-in. slab caused by 12-kip single-axle load 4 ft from joint. Loop 1.

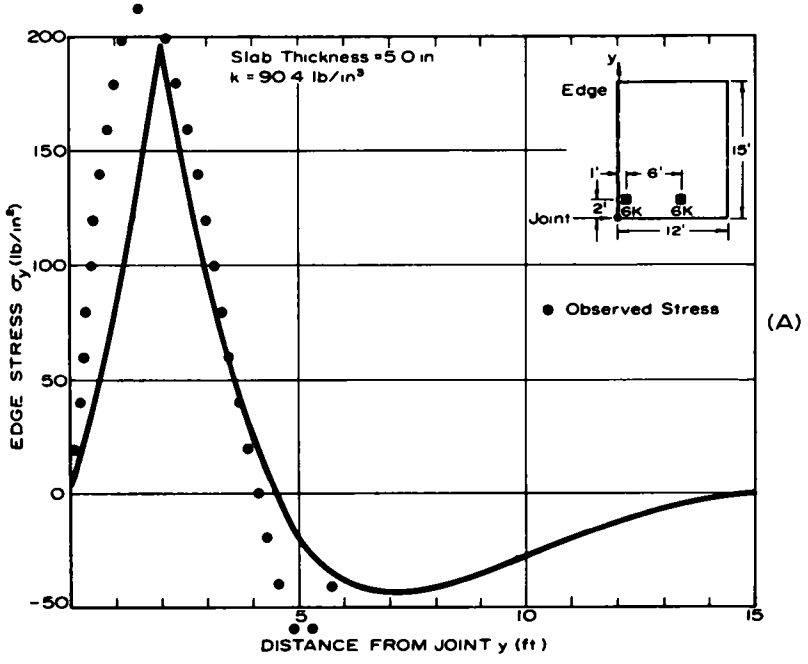

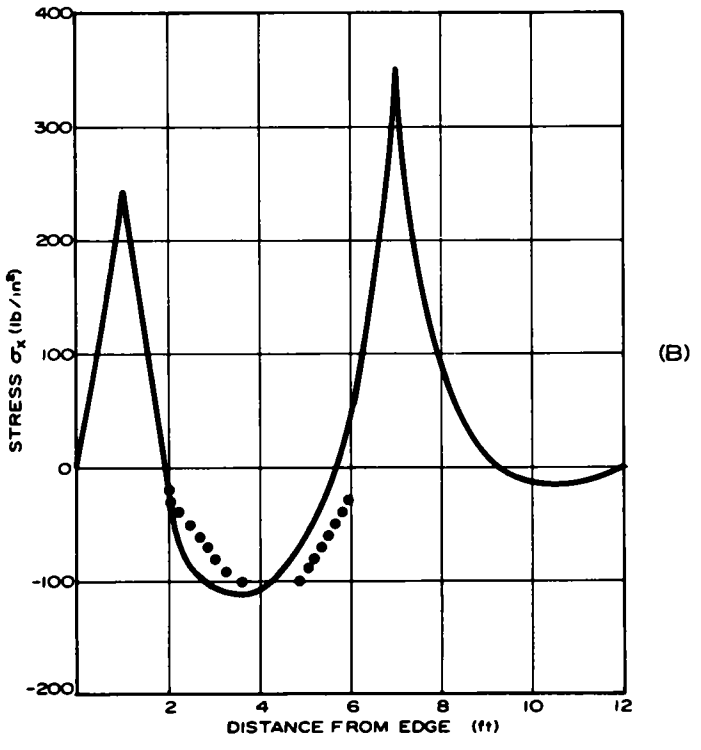

Figure 18. Stresses in 5.0-in. slab caused by 12-kip single-axle load 2 ft from joint; Loop 1.

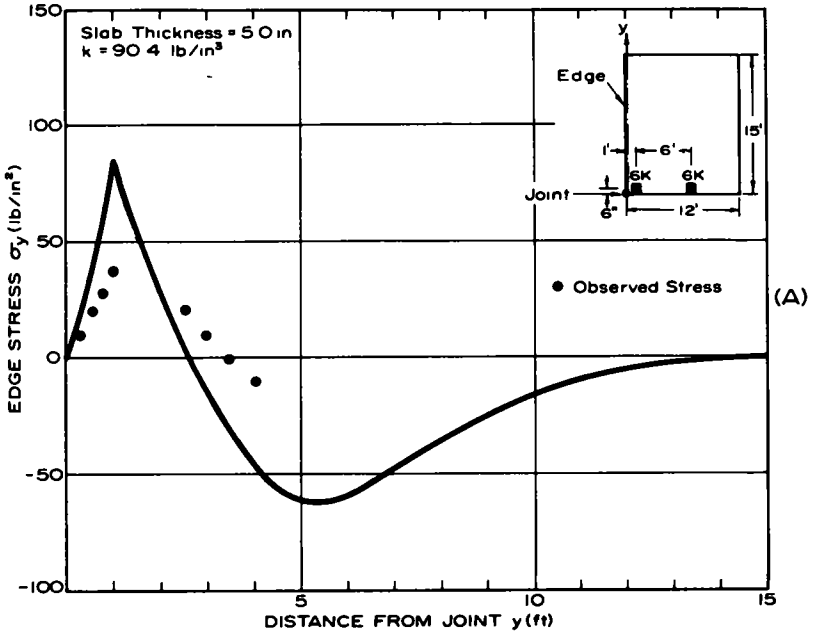

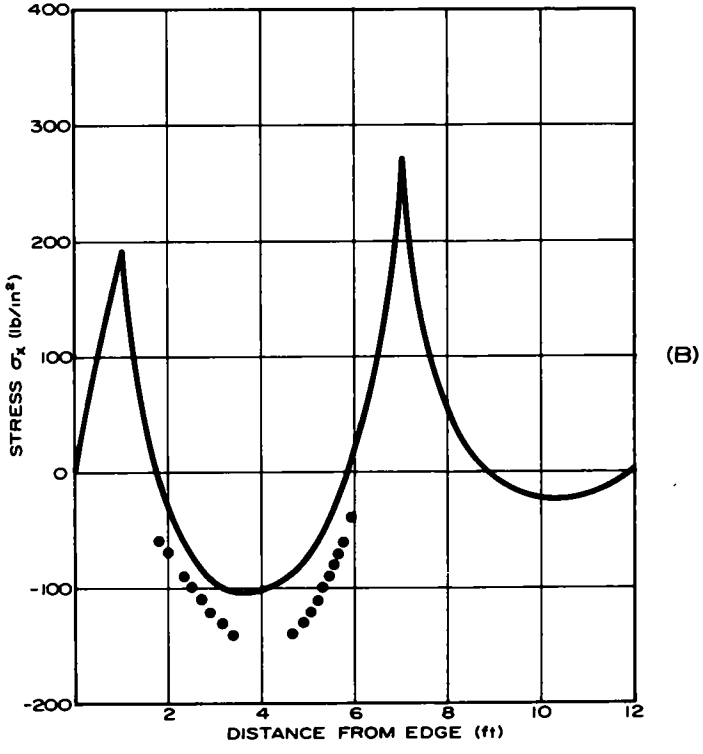

Figure 19. Stresses in 5.0-in. slab caused by 12-kip single-axle load 6 in. from joint, Loop 1.

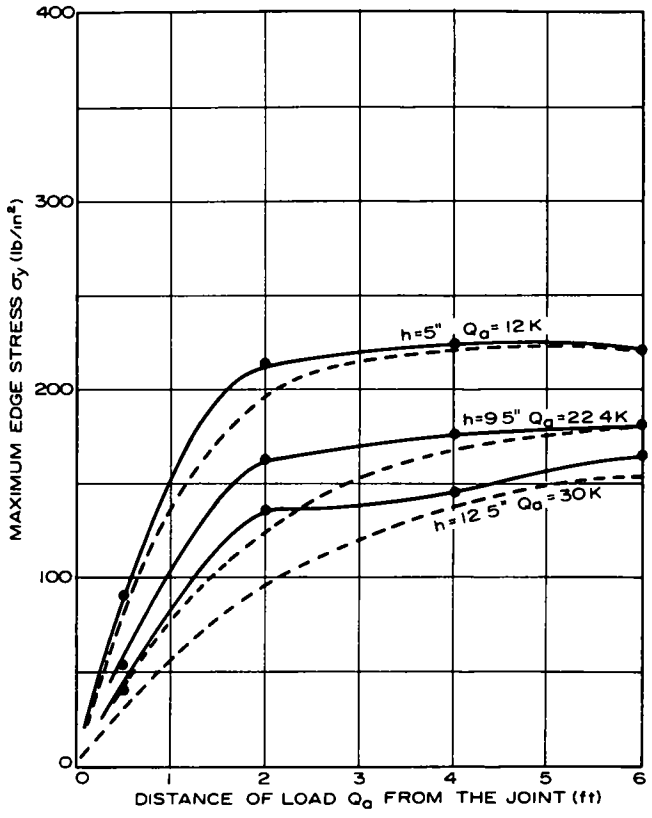

Figure 20 Maximum edge stress vs distance of single-axle load from joint, Loop 1

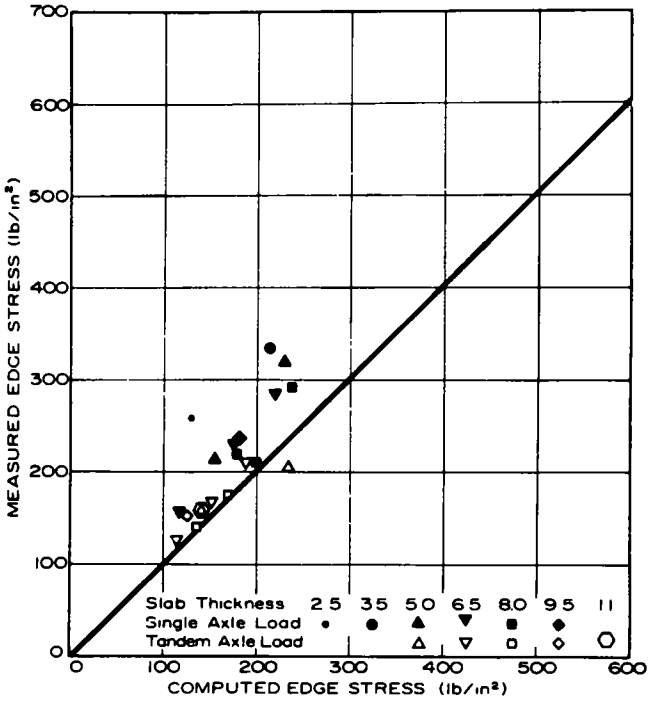

Figure 21 Comparison of measured and computed edge stresses, main loops

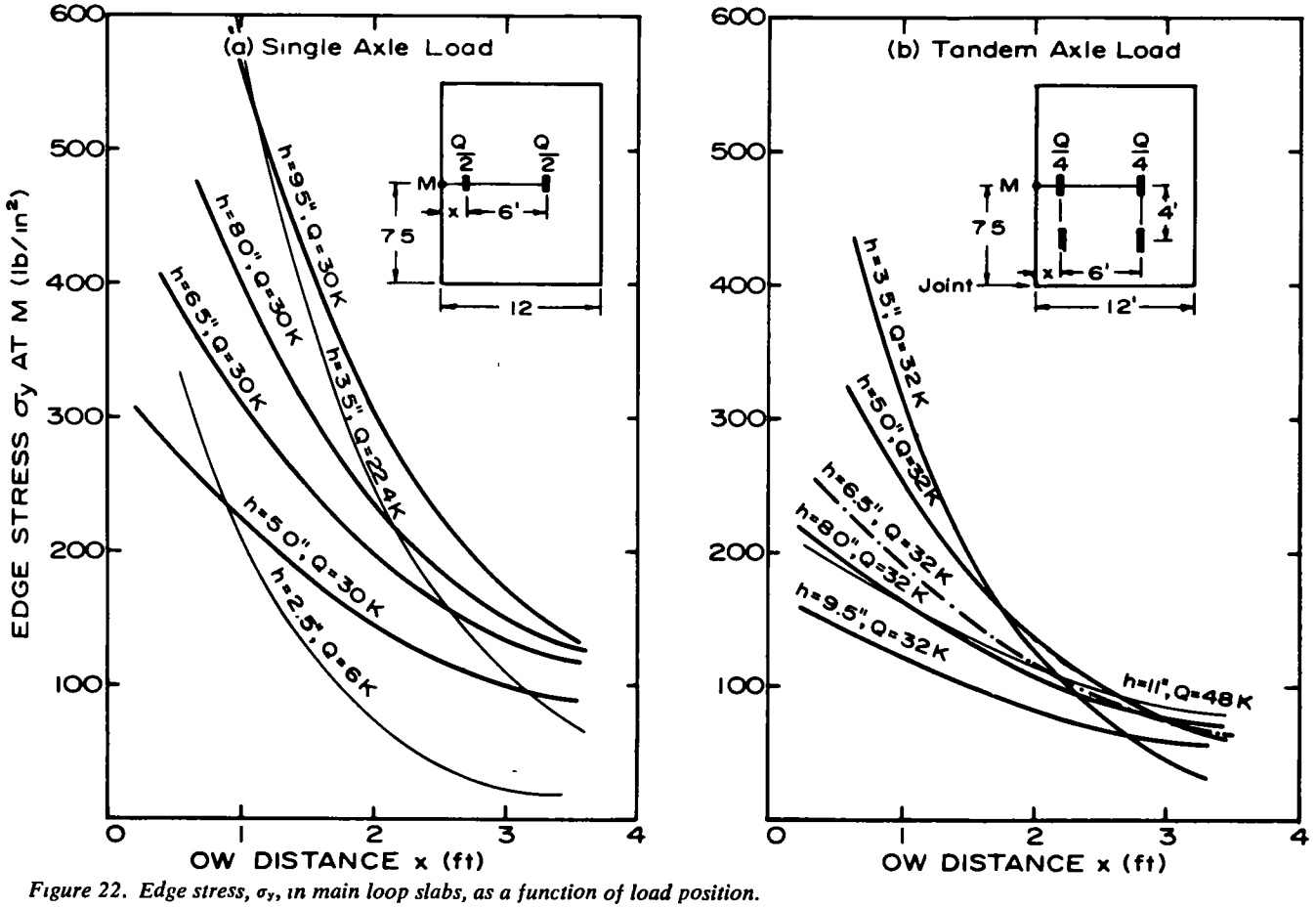

Figure 22. Edge stress, σ_y, in main loop slabs, as a function of load position.

TABLE 10

COMPARISON OF MEASURED AND COMPUTED DEFLECTIONS

LOOP NO	AXLE LOAD, Q (KIPS)	SLAB THICKNESS, h (IN)	SUBBASE THICKNESS (IN)	DEFLECTION (IN) MEASURED CORNER	MEASURED EDGE	COMPUTED CORNER	COMPUTED EDGE
4	18–S	6 5	3	0 026	0 020	0 080	0.048
			3	0 027	0 026		
			3	0 024	0.020		
			6	0.025	0 016		
	32–T	6 5	3	0 024	0.018	0.062	0.054
			9	0 032	0 018		
			3	0 024	0 016		
			3	0 026	0 024		
			6	0 031	0 030		
			9	0 025	0.020		
5	22 4–S	8 0	3	0.035	0 031	0 051	0 050
			6	0 032	0 034		
			3	0 028	0.022		
			3	0 047	0 038		
	40–T	8 0	3	0 036	0 028	0 106	0 073
			6	0.031	0 026		
			6	0 029	0 026		
			9	0 028	0 024		
			3	0 034	0 024		
			3	0 033	0 030		
			6	0 030	0 040		
			9	0 034	0 032		

PAVEMENT PERFORMANCE AND MODES OF FAILURE

The principal design criterion of most known theories of structural design of rigid pavements is based on considerations of tensile stress, σ, in the pavement slab. The slab thickness, h, is selected so as to keep this stress within certain limits, set by the ultimate tensile strength, f_c, of the slab material in bending. Such an approach, following the basic philosophy used generally in structural design, is not entirely satisfactory as long as it does not take into account the pavement serviceability. It is well known that a pavement may exhibit failure in the classical sense of structural mechanics and still perform its function

One of the major developments resulting from the AASHO Road Test has been the introduction of an index of performance known as "present serviceability index," p. Unfortunately, in most analyses of AASHO Road Test data, this index has been related to wheel loads and pavement thicknesses on a purely empirical basis, though with elaborate statistical analyses. The only exception to this is found in an attempt by Hudson and Scrivner (*40*) to relate the rigid pavement performance directly to the edge stress, σ_y, measured in the main loops. They investigated the relationship between edge stress, σ_y, and the number of load repetitions, $N_{2.5}$, needed to reduce the serviceability index to 2.5 and found that σ_y may not provide a good absolute measure of pavement performance. However, they derived, at the same time, two different relationships that were statistically satisfactory for single and tandem loads, respectively. They concluded that the edge stress was probably not the critical stress for slabs subjected to tandem loads and expressed the hope that a general correlation of the kind could be developed by using appropriate analysis.

With this purpose in mind, a complete stress and deflection analysis was performed for all rigid pavement slabs of the AASHO Road Test for which the serviceability data were available. The basic data about the analyses performed are given in Tables 11 and 12. Principal results are also given in these tables; in particular, maximum value of stress components σ_x and σ_y, as well as of the principal stress differences $(\sigma_1 - \sigma_3)$ for different positions of the axle loads along the slab panels. The variations of maximum values of σ_x, σ_y, and $(\sigma_1 - \sigma_3)$ with the position of the loads on the slab panels are also shown graphically in Figures 23 through 28.

Study of the results presented in the mentioned tables and figures leads to several interesting observations. Firstly, it is seen that critical stresses for thin slabs are generally σ_x-stresses along the wheel paths, whereas the critical stresses for thicker slabs are generally σ_y-stresses occurring under the wheels positioned around the middle of the slab panels. This observation explains very nicely the crack patterns observed in the AASHO Test Road (Figs. 29 and 30). In the case of 3.5-in. slab loaded by 24-kip tandem load (Fig. 29) first cracks appear near the joints, where, according to analysis (Fig. 26) the highest combined stresses occur. The crack further develops along the

TABLE 11

MAXIMUM COMPUTED STRESSES IN MAIN LOOP UNDER SINGLE LOADS

SLAB THICKNESS, h (IN.)	AXLE LOAD, Q (KIPS)	DISTANCE OF WHEELS (FT)	MAXIMUM σ_x MAGNITUDE (LB/IN.^{2})	POSITION	MAXIMUM σ_y MAGNITUDE (LB/IN.^{2})	POSITION	MAXIMUM $(\sigma_1-\sigma_3)$ MAGNITUDE (LB/IN.^{2})	POSITION
2.5	6	0	448	(8.5,0)	498	(2.5,0)	292	(2.5,1)
		1	577	(8.5,1)	547	(2.5,1)	186	(3.5,1)
		2	550	(8.5,2)	559	(2.5,2)	192	(2.5,2)
		3	545	(8.5,3)	556	(2.5,3)	192	(2.5,3)
		4	544	(8.5,4)	554	(2.5,4)	189	(2.5,4)
		5	544	(8.5,5)	554	(2.5,5)	189	(2.5,5)
		7	544	(8.5,7)	554	(2.5,7)	189	(2.5,7)
3.5	22.4	0	1100	(8.5,1)	−1180	(2.5,1)	1655	(2.5,1)
		1	1425	(8.5,1)	1030	(2.5,1)	606	(8.5,1)
		2	1240	(8.5,2)	1280	(2.5,2)	504	(3,2)
		3	1215	(8.5,3)	1315	(2.5,3)	524	(3,3)
		4	1200	(8.5,4)	1300	(2.5,4)	512	(3,4)
		5	1195	(8.5,5)	1290	(2.5,5)	500	(3,5)
		7	1195	(8.5,7)	1280	(2.5,7)	492	(3,7)
5	30	0	844	(8.5,1)	−844	(2.5,−1)	1240	(8.5,1)
		1	1030	(8.5,1)	710	(2.5,1)	583	(8.5,−1)
		2	897	(8.5,2)	960	(2.5,2)	418	(3.5,2)
		3	883	(8.5,3)	1065	(2.5,3)	498	(3,3)
		4	880	(8.5,4)	1100	(2.5,4)	522	(3,4)
		5	876	(8.5,5)	1095	(2.5,5)	525	(3,5)
		7	873	(8.5,7)	1080	(2.5,7)	513	(3,7)
6.5	30	0	522	(8.5,1)	−512	(2.5,−1)	767	(8.5,1)
		1	629	(8.5,1)	426	(2.5,1)	371	(8.5,−1)
		2	546	(8.5,2)	594	(2.5,2)	263	(3.5,2)
		3	539	(8.5,3)	683	(2.5,3)	336	(3,3)
		4	538	(8.5,4)	725	(2.5,4)	374	(3,4)
		5	539	(8.5,5)	742	(2.5,5)	389	(3,5)
		7	538	(8.5,7)	742	(2.5,7)	390	(3,7)
8.0	30	0	357	(8.5,1)	−343	(2.5,−1)	524	(8.5,1)
		1	424	(8.5,1)	285	(2.5,1)	259	(8.5,−1)
		2	368	(8.5,2)	407	(2.5,2)	183	(3.5,2)
		3	363	(8.5,3)	484	(2.5,3)	249	(3,3)
		4	364	(8.5,4)	531	(2.5,4)	292	(3,4)
		5	365	(8.5,5)	556	(2.5,5)	317	(1,5)
		7	365	(8.5,7)	566	(2.5,7)	326	(1,7)
9.5	30	0	254	(8.5,1)	−245	(2.5,−1)	374	(8.5,1)
		1	301	(8.5,1)	202	(2.5,1)	186	(8.5,−1)
		2	260	(8.5,2)	290	(2.5,2)	131	(3.5,2)
		3	258	(8.5,3)	348	(2.5,3)	180	(3,3)
		4	259	(8.5,4)	384	(2.5,4)	219	(3,4)
		5	259	(8.5,5)	407	(2.5,5)	234	(1,5)
		7	259	(8.5,7)	412	(2.5,7)	243	(1,7)

outer wheel path, where, according to analysis, the higher stresses, σ_x, are found in the transverse direction. Contrary to this, in the case of an 8-in slab loaded by 30-kip single-axle load (Fig. 30), the first cracks appear near the middle of the slab panels. These cracks are in the transverse direction, exactly where the analysis (Fig. 25) shows the highest σ_y stresses. Some cracking appears later in the vicinity of the joints to reflect the presence of high principal stress differences, $\sigma_1 - \sigma_3$.

Secondly, if the critical stresses for each loading case and slab are plotted versus the number of load repetitions, $N_{2.5}$, needed to reduce the serviceability index to 2.5, *a unique relationship results for all slabs, regardless of type of loading* (Fig. 31).

This most significant finding confirms the soundness of a rational, mechanistic approach to design of rigid pavements. It demonstrates beyond doubt that failure in pavement performance is not a phenomenon of chance, as some statistical approaches tend to suggest, but a phenomenon that has a definite mechanical cause.

It can be shown that the data in Figure 31 can be fitted by

$$N_{2.5} = 225{,}000\,(f_c/\sigma)^4 \qquad (17)$$

TABLE 12

MAXIMUM COMPUTED STRESSES IN MAIN LOOP UNDER TANDEM LOADS

SLAB THICKNESS, h (IN.)	AXLE LOAD, Q (KIPS)	DISTANCE OF FIRST WHEEL, y (FT)	MAXIMUM σ_x MAGNITUDE (LB/IN.^{2})	POSITION		MAXIMUM σ_y MAGNITUDE (LB/IN.^{2})	POSITION		MAXIMUM $(\sigma_1-\sigma_3)$ MAGNITUDE (LB/IN.^{2})	POSITION	
3.5	32	−2	895	(3,−2)	(3,2)	816	(3,−2)	(3,+2)	399	(3,−1)	(9,−1)
		−1	964	(3,−1)	(9,−1)	786	(3,3)	(9,3)	513	(3,1)	(9,1)
		0[a]	881	(3,4)	(9,4)	752	(3,5)	(9,5)	1280	(3,1)	(9,1)
		1	1050	(3,1)	(9,1)	812	(3,5)	(9,5)	516	(3,−1)	(9,−1)
		2	905	(3,2)	(9,2)	838	(3,2)	(9,2)	352	(3,4)	(9,4)
		3	879	(3,3)	(9,3)	847	(3,3)	(9,3)	348	(3,5)	(9,5)
		4	869	(3,4)	(9,4)	831	(3,4)	(9,4)	351	(3,5)	(9,5)
5	32	−2	482	(3,2)	(9,2)	409	(3,2)	(9,2)	239	(3,−1)	(9,−1)
		−1	514	(3,−1)	(9,−1)	410	(3,3)	(9,3)	293	(3,1)	(9,1)
		0[a]	506	(3,1)	(9,1)	389	(3,4)	(9,4)	695	(3,1)	(9,1)
		1	575	(3,1)	(9,1)	480	(3,5)	(9,5)	327	(3,−1)	(9,−1)
		2	498	(3,2)	(9,2)	513	(3,6)	(9,6)	217	(6,2)	
		3	487	(3,3)	(9,3)	543	(3,7)	(9,7)	232	(6,3)	
		4	482	(3,4)	(9,4)	546	(3,4)	(9,4)	231	(6,4)	
6.5	48	−2	441	(3,2)	(9,2)	357	(3,2)	(9,2)	229	(3,−1)	(9,−1)
		−1	471	(3,−1)	(9,−1)	367	(3,3)	(9,3)	272	(3,1)	(9,1)
		0[a]	473	(3,1)	(9,1)	355	(3,4)	(9,4)	631	(3,1)	(9,1)
		1	527	(3,1)	(9,1)	473	(3,5)	(9,5)	318	(3,−1)	(9,−1)
		2	458	(3,2)	(9,2)	532	(3,6)	(9,6)	216	(1,6)	(11,6)
		3	450	(3,3)	(9,3)	562	(3,7)	(9,7)	258	(6,3)	
		4	448	(3,4)	(9,4)	578	(3,4)	(9,4)	274	(6,4)	
8	48	−2	299	(3,2)	(9,2)	231	(3,2)	(9,2)	161	(3,−1)	(9,−1)
		−1	319	(3,−1)	(9,−1)	245	(3,3)	(9,3)	186	(3,1)	(9,1)
		0[a]	325	(3,1)	(9,1)	244	(3,4)	(9,4)	437	(3,−1)	(9,−1)
		1	356	(3,1)	(9,1)	350	(3,5)	(9,5)	227	(3,−1)	(9,−1)
		2	310	(3,2)	(9,2)	414	(3,6)	(9,6)	201	(1,6)	(11,6)
		3	306	(3,3)	(9,3)	450	(3,7)	(9,7)	234	(1,7)	(11,7)
		4	307	(3,4)	(9,4)	461	(3,8)	(9,8)	247	(1,8)	(11,8)
9.5	48	−2	212	(3,2)	(9,2)	162	(3,+2)	(9,+2)	115	(3,−1)	(9,−1)
		−1	227	(3,−1)	(9,−1)	173	(3,2)	(9,2)	128	(3,−4)	(9,−4)
		0[a]	231	(3,1)	(9,1)	174	(3,4)	(9,4)	313	(3,−1)	(9,−1)
		1	253	(3,1)	(9,1)	253	(3,5)	(9,5)	163	(3,−1)	(9,−1)
		2	220	(3,2)	(9,2)	303	(3,6)	(9,6)	151	(1,6)	(11,6)
		3	218	(3,3)	(9,3)	307	(3,7)	(9,7)	178	(1,7)	(11,7)
		4	218	(3,4)	(9,4)	340	(3,8)	(9,8)	187	(1,8)	(11,8)
11	48	−2	161	(3,4)	(9,4)	117	(3,2)	(9,2)	91	(3,−1)	(9,−1)
		−1	172	(3,−1)	(9,−1)	130	(3,3)	(9,3)	114	(3,−4)	(9,−4)
		0[a]	177	(3,1)	(9,1)	136	(3,4)	(9,4)	243	(3,−1)	(9,−1)
		1	191	(3,1)	(9,1)	209	(3,5)	(9,5)	130	(3,−1)	(9,−1)
		2	167	(3,2)	(9,2)	258	(3,6)	(9,6)	144	(1,6)	(11,6)
		3	168	(3,7)	(9,7)	287	(3,7)	(9,7)	172	(1,7)	(11,7)
		4	167	(3,8)	(9,8)	296	(3,8)	(9,8)	181	(1,8)	(11,8)

[a] Joint

in which f_c represents, as before, tensile strength of the pavement slab material in bending. (For AASHO slabs, $f_c = 790$ lb/in.^{2}, see Table 4.)

It is important to remember that σ represents the maximum *combined* tensile stress in the pavement slab caused by traffic load, Q, moving in the anticipated *average* wheel path position. (In existing design procedures σ is computed as the absolute maximum stress caused by loads placed in some *extreme* positions such as slab edge or slab corner.)

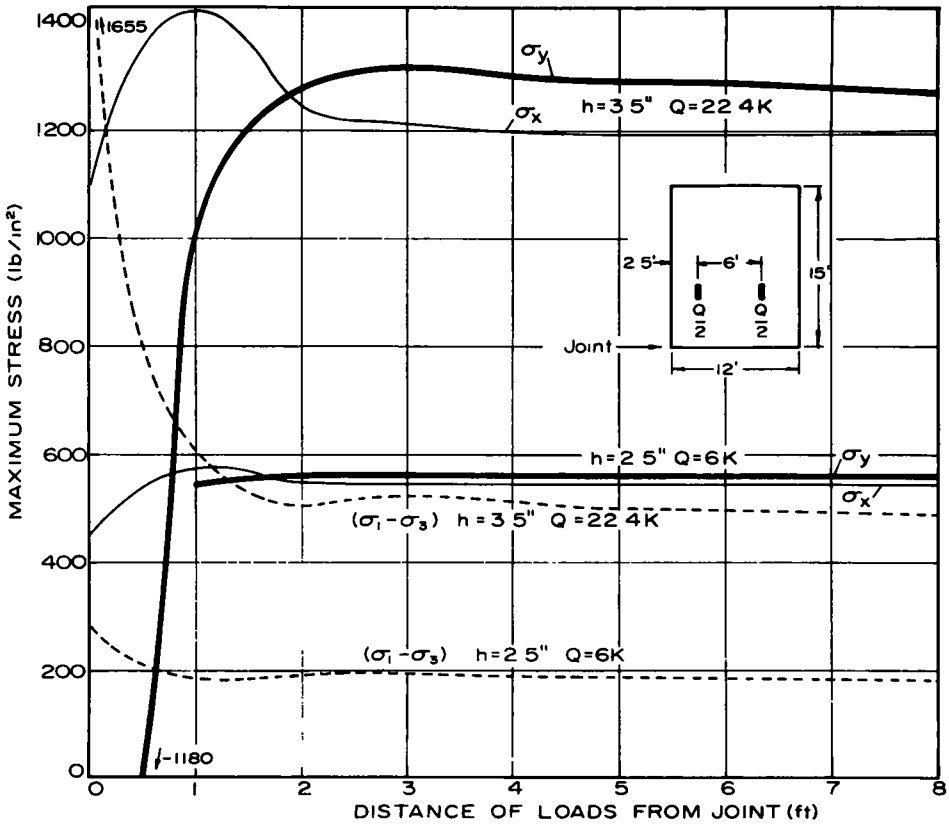

Figure 23. Computed maximum stresses in main loop slabs 2 5 and 3 5 in. thick (single loads)

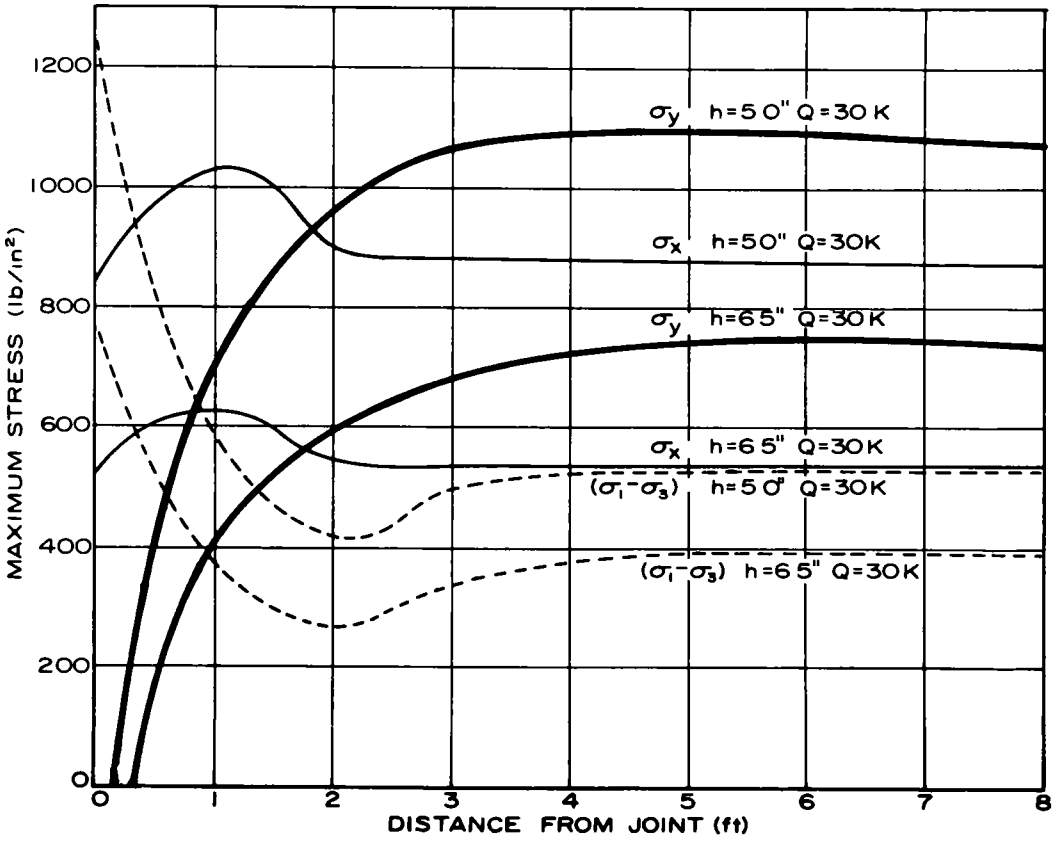

Figure 24 Computed maximum stress in main loop slabs 5 and 6 5 in. thick (single loads).

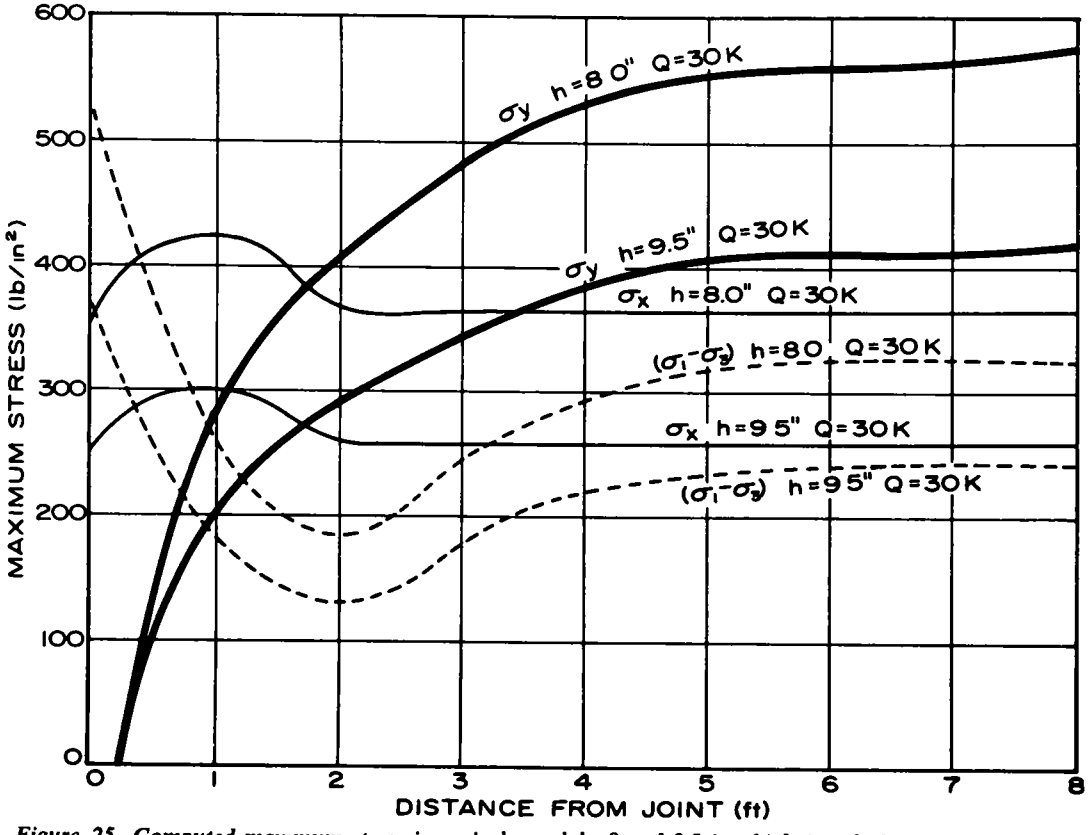

Figure 25. Computed maximum stress in main loop slabs 8 and 9.5 in. thick (single loads).

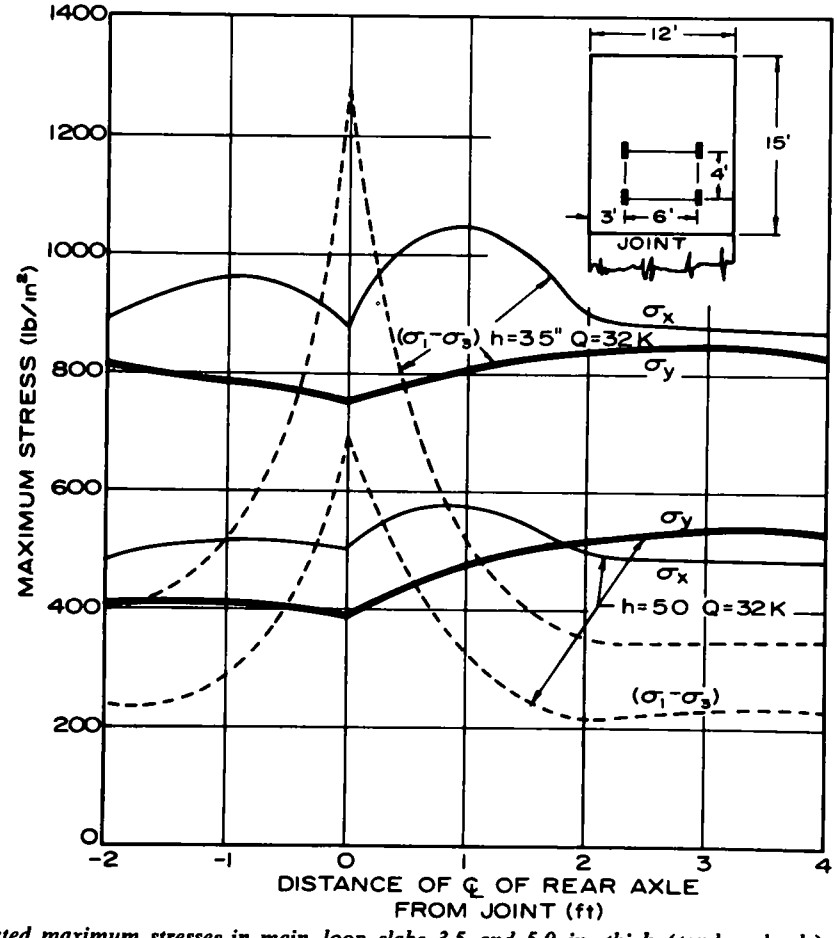

Figure 26. Computed maximum stresses in main loop slabs 3.5 and 5.0 in. thick (tandem loads).

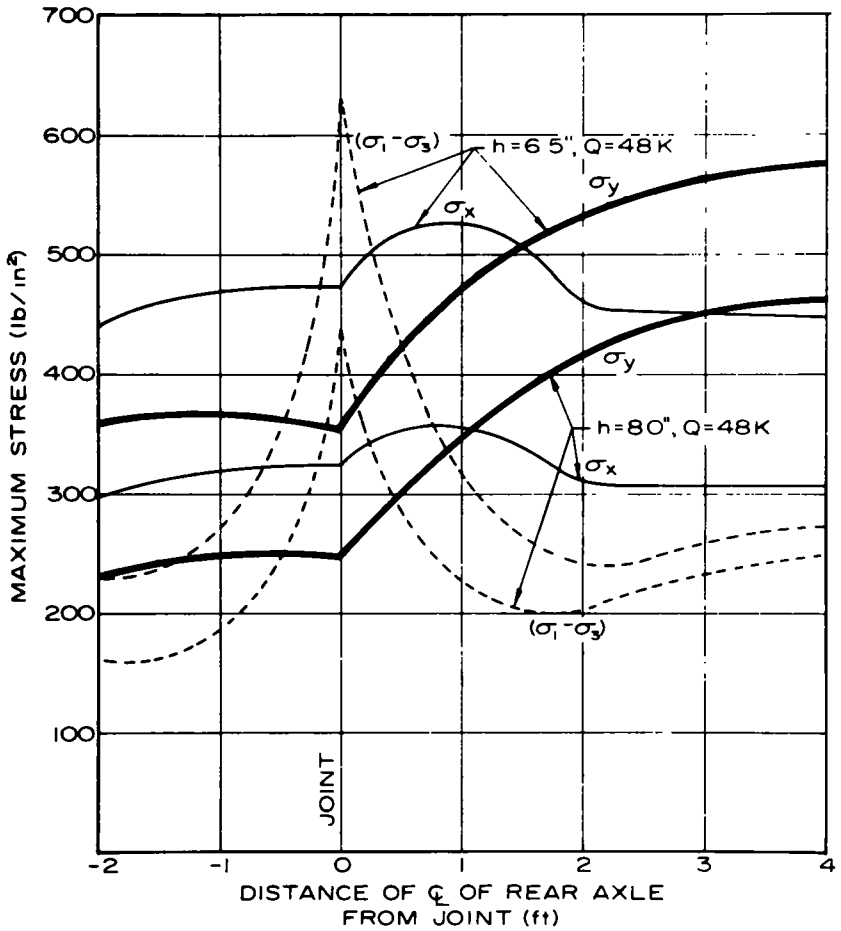

Figure 27 Computed maximum stresses in main loop slabs 6.5 and 8 0 in thick (tandem loads)

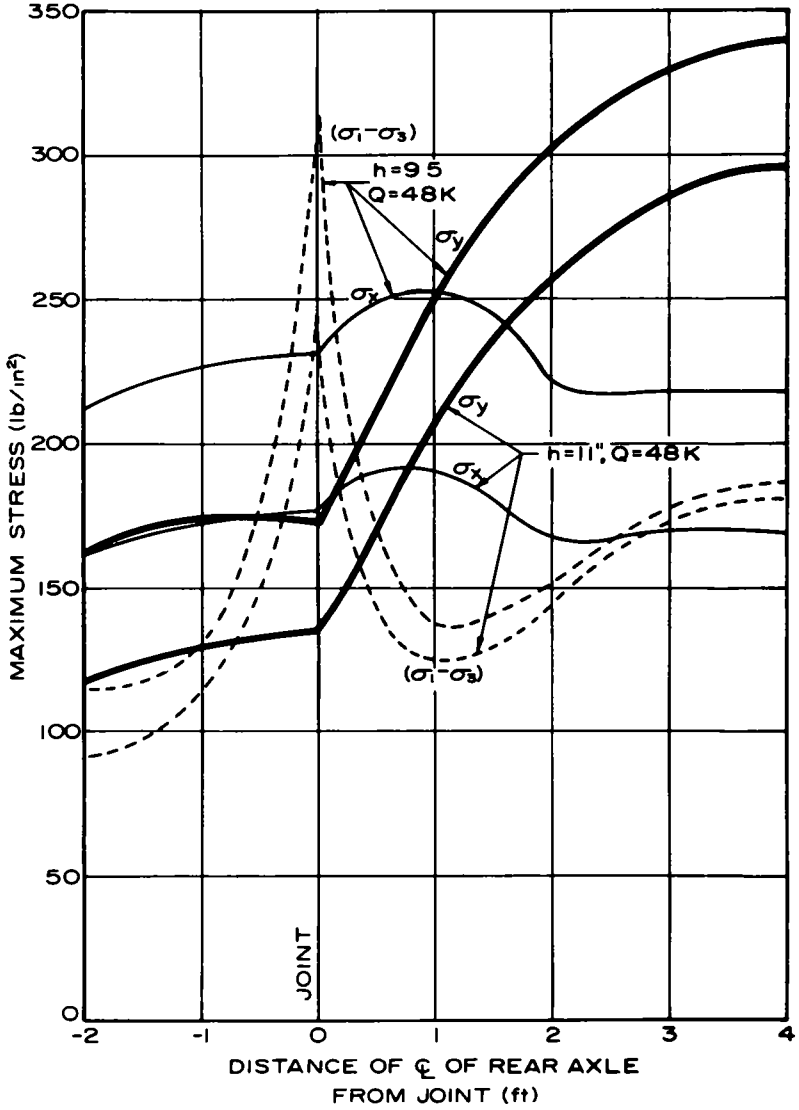

Figure 28. Computed maximum stresses in main loop slabs 9.5 and 11 0 in. thick (tandem loads).

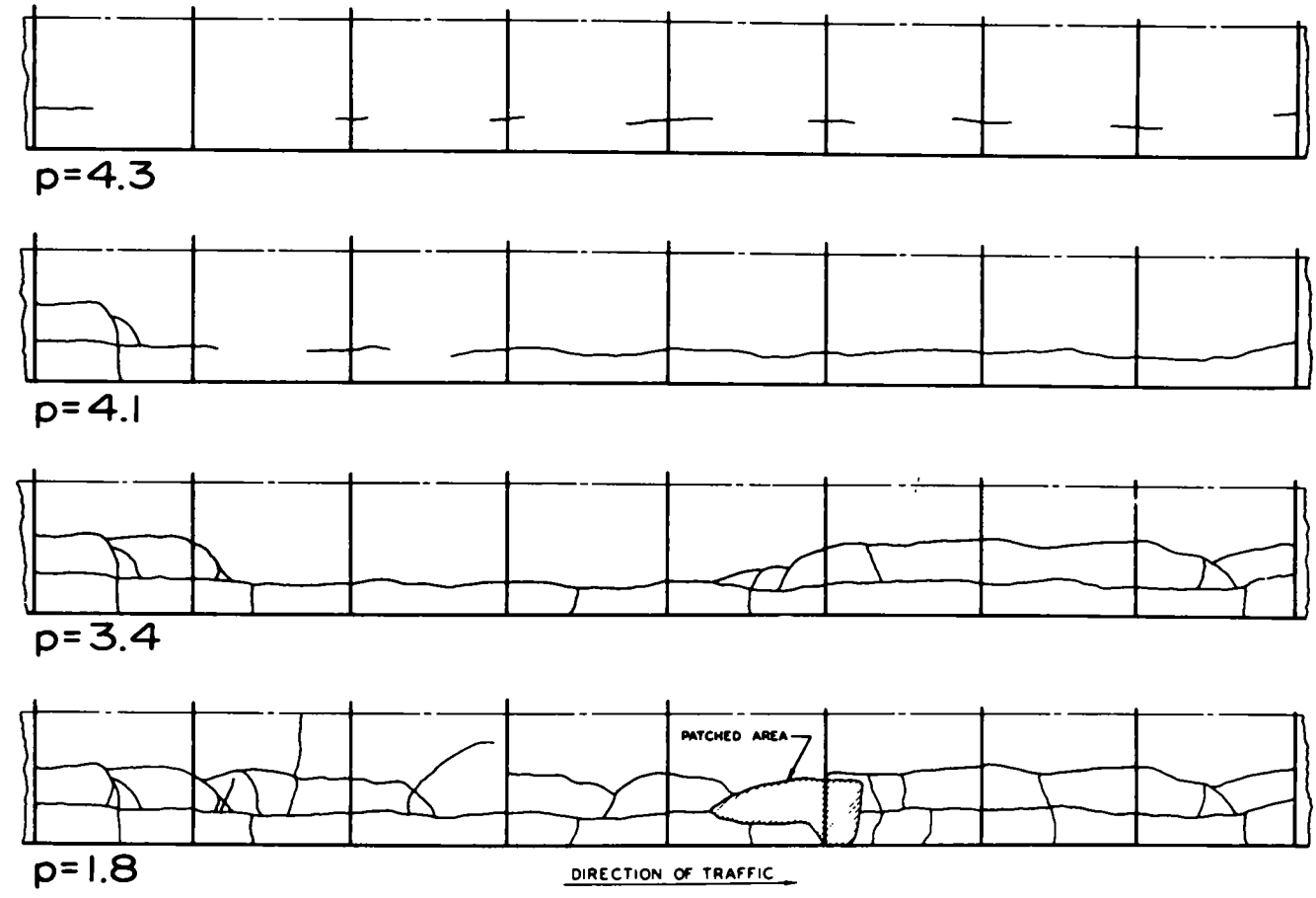

Figure 29. Progression of crack pattern in a 3 5-in slab under 24-kip tandem-axle load (after Ref. 39)

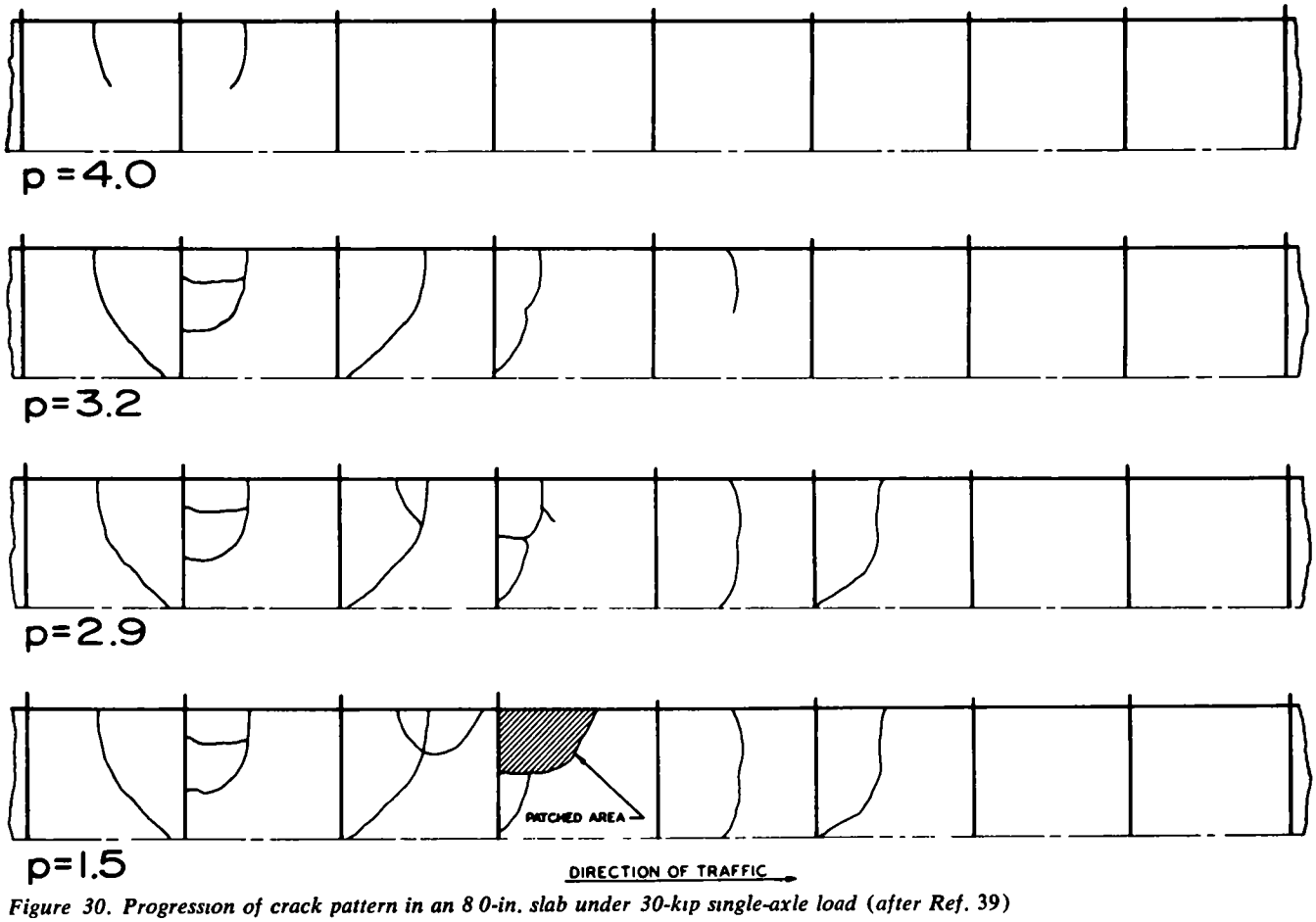

Figure 30. Progression of crack pattern in an 8 0-in. slab under 30-kip single-axle load (after Ref. 39)

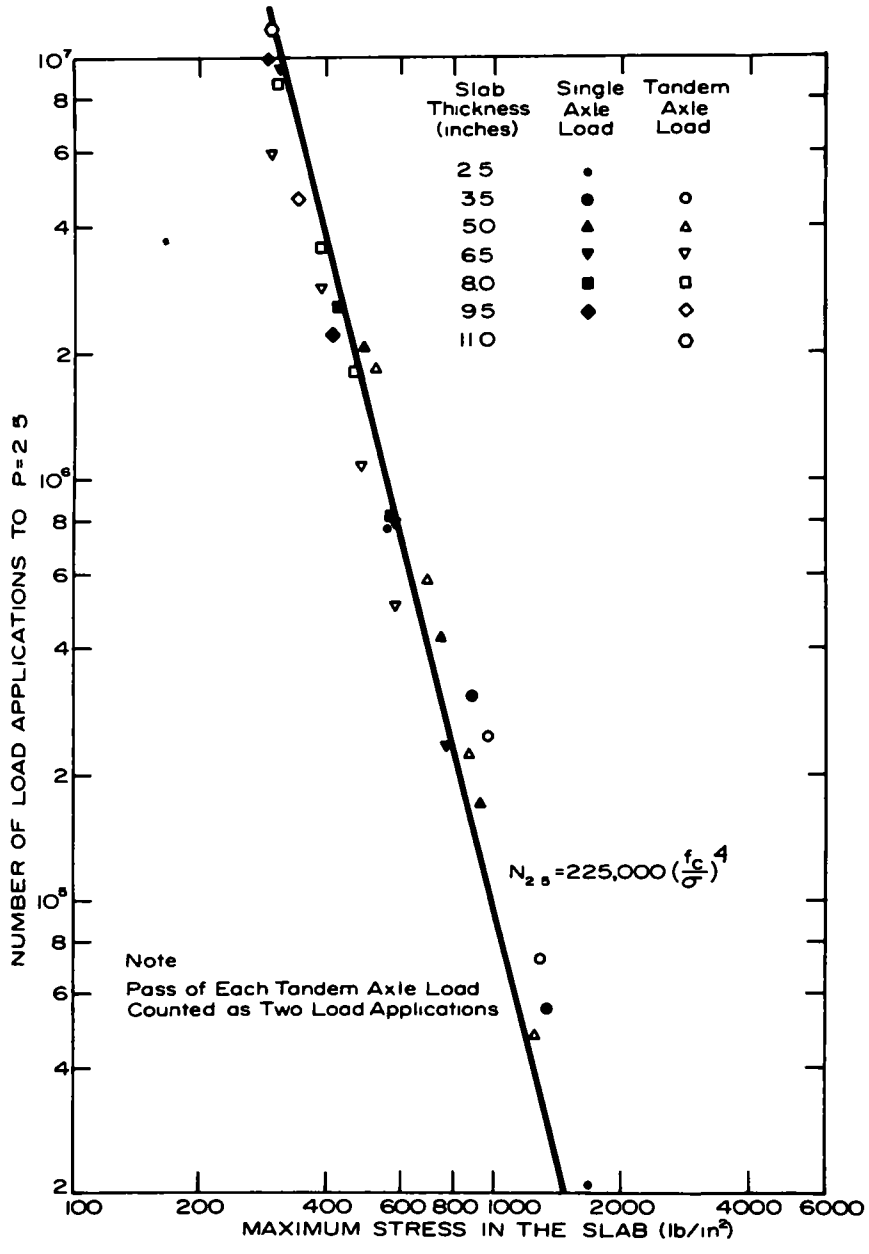

Figure 31 Relationship of performance to main loop compressive edge stresses (computed).

CHAPTER FOUR

APPLICATIONS, CONCLUSIONS, AND RECOMMENDATIONS

IMPLICATIONS FOR DESIGN

Chapter One is devoted to a critical review of existing theories of structural behavior of rigid pavements. These theories differ principally in the model selected to represent the subgrade supporting the pavement slab. Two principal models are being used—the elastic-isotropic solid, characterized by a modulus of deformation, E_s, and a Poisson's ratio, ν_s, and the Winkler subgrade, characterized by a coefficient of subgrade reaction, k

It is shown that, with a suitable selection of coefficient k, theories based on the Winkler model for the subgrade can furnish adequate answers also for slabs resting on a subgrade behaving as an elastic solid. However, there is no single value of k that can give perfect agreement of all statical influences in a particular case, unless the subgrade thickness is limited to a maximum of 2 5 stiffness radii of the slab. The following analytical expressions are presented for evaluation of k for a slab of thickness h and with deformation characteristics E, ν, resting on a subgrade of depth H, with deformation characteristics E_s, ν_s:

(a) Subgrade of infinite depth $(H \to \infty)$

$$k_0 = 0.91 \sqrt[3]{\frac{E_s (1-\nu^2)}{E (1-\nu_s^2)}} \frac{E_s}{(1-\nu_s^2)\, h^2} \qquad (8)$$

In simplified form,

$$k_0 = \sqrt[3]{\frac{E_s}{E}} \frac{E_s}{(1-\nu_s^2)\, h^2} \qquad (9)$$

(b) Subgrade of finite depth $\left(H \leq 1.38 \sqrt[3]{\frac{E}{E_s}}\, h\right)$

$$k_0' = 1.38 \frac{E_s}{(1-\nu_s^2)\, H^2} \qquad (14)$$

The existence of a unique relationship, such as Eq. 17, for all rigid pavements of the AASHO Road Test has additional general implications regarding rigid pavement design. Considering the fact that the pavement stress, σ, is found to be proportional to wheel load, Q, and inversely proportional approximately to the 1.25 power of the slab thickness, h (*39E*, p. 192) the following general relationship between principal variables in the AASHO Road Test can be established:

$$N_{2\,5} = C\, f_c^4\, h^5\, Q^{-4} \qquad (18)$$

in which C is a constant.

This equation suggests that slab thickness should be increased as the fifth root of the anticipated number of load applications. This means, for example, that under otherwise equal circumstances the pavement life may be increased 1 8 times by adopting 9-in. instead of 8-in. slab thickness, and 3 times by adopting 10-in. instead of 8-in. slab thickness. At the same time the pavement life can be reduced to one-half by adopting 7-in. instead of 8-in. slab thickness.

It also follows from Eq. 18 that the AASHO pavement life varied as the fourth power of the concrete strength. This points out the importance of quality of materials in pavement construction: a 10 percent increase in strength may mean 50 percent increase in pavement life, and a 20 percent increase in strength may mean doubling the pavement life. At the same time, a 10 percent reduction in concrete strength may mean reducing the pavement life to 65 percent of the normal expectation, and a 20 percent reduction in strength may mean reducing the life to 40 percent of the normal expectation.

Eq 18 may give a rational basis for evaluation of effects of overload and mixed traffic on pavement life. A consistent 10 percent overload may reduce the pavement life almost 1.5 times; a consistent 20 percent overload may reduce the pavement life to one-half the normally expected time. One application of double load is equivalent to 16 applications of normal load; at the same time, 16 applications of the half-load in a mixed traffic should be equivalent to one application of normal load. Also, 6,500 applications of a 2-kip axle load should be equivalent to one application of an 18-kip axle load.

The analyses leading to Eq. 17 furnish also a rational basis for evaluation of equivalency of single and tandem loads under much more general conditions than was possible in the past With such an expression it becomes possible to predict in a rational way what would be the effect of using, on a certain pavement, tandem axle loads with different axle spacing or with a different distance between extreme wheels. Moreover, it becomes possible to predict with somewhat greater certainty the potential life of a rigid pavement subjected to traffic by a new vehicle, which may be of entirely different characteristics than any other vehicle used in the past on similar pavements. Thus, the theoretical findings presented in this study have a potentially great practical importance.

CONCLUSIONS

The principal conclusions reached in this research project can be summarized as follows:

1. Failure in rigid pavement performance is not a phenomenon of chance, as some statistical approaches tend to suggest, but a phenomenon that has a definite mechanical cause. The results of this study confirm that the tensile stress in the pavement slab caused by the moving loads represents the best indicator of pavement performance. This finding lends support to the basic design philosophy of most existing theoretical methods of rigid pavement design.
2. The over-all response of the AASHO subgrade to

loads transmitted through the pavement slabs can be adequately simulated by the response of an ideal homogeneous, isotropic, elastic (Hookean) solid, represented by two deformation characteristics—modulus of deformation, E_s, and Poisson's ratio, ν_s. A reasonable simulation of subgrade response can also be achieved by using the Winkler model, represented by a coefficient of subgrade reaction, k (used in the well-known Westergaard theory). However, there is no single value of k that can yield perfect agreement of all statical influences such as bending moments, shearing forces, contact pressures, and deflections.

3. A simple relationship (Eq 8) has been derived to correlate the coefficient of subgrade reaction, k, that gives good agreement of bending moments across the slab with deformation characteristics of the subgrade and the slab material. This relationship suggests that the coefficient of subgrade reaction, k, for a particular location, such as that of the AASHO Road Test, should not be a constant depending on the soil type only, but a variable quantity that is inversely proportional to the slab thickness, h. This important finding is confirmed by many measurements and observations made in the AASHO Road Test.

4. The over-all suitability of the Winkler subgrade model for analysis of rigid pavement slabs is better if the compressible subgrade extends to a limited depth under the pavement slab. As long as the depth of compressible subgrade remains smaller than about 2.5 stiffness radii of the slab, it is possible to find a single value of k (given by Eq 14) that will yield good agreement of all statical influences, including both stresses and deflections of the slab.

5. Eq. 18, relating the ultimate number of axle-load applications, $N_{2.5}$, to the flexural strength of pavement material, f_c, thickness of pavement slab, h, and the magnitude of axle load, Q, suggests that the pavement life should increase in proportion to the fourth power of strength of slab material, and to the fifth power of slab thickness. At the same time the pavement life should decrease in inverse proportion to the fourth power of the axle load. Eq. 18 offers a new rational basis for evaluation of an equivalent number of axle-load applications for rigid pavements subjected to mixed traffic.

SUGGESTED RESEARCH

In the light of findings of this investigation it would be highly desirable to develop rapid procedures for evaluation of stresses in pavement slabs resting on an elastic-isotropic solid and subjected to arbitrary surface loads. In view of the widespread use of the Westergaard theory, additional experimental verifications of dependence of the coefficient of subgrade reaction, k, on slab dimensions and thickness of the compressible subgrade are also needed, preferably from large-scale model or full-scale tests under carefully controlled conditions. Most of all, additional observations of relationships between principal parameters affecting rigid pavement performance in actual field conditions would be of great interest.

REFERENCES

1. GOLDBECK, A T., "Thickness of Concrete Slabs." *Pub. Roads,* pp. 34-38 (June 1919)
2. GOLDBECK, A. T., "Researches on the Structural Design of Highways by the United States Bureau of Public Roads" *Trans. ASCE,* Vol. 88, Paper No. 1557, pp. 264-300 (1925)
3. OLDER, C., "Highway Research in Illinois." *Trans. ASCE,* Vol. 87, Paper No. 1546, pp. 1180-1224 (1924)
4. WESTERGAARD, H. M., "Stresses in Concrete Pavement Computed by Theoretical Analysis." *Pub. Roads,* Vol 7, No. 2, pp. 25-35 (1926).
5. WESTERGAARD, H. M., "Analysis of Stresses in Concrete Roads Caused by Variations of Temperature." *Pub. Roads,* Vol. 8, No. 3, pp. 54-60 (1927).
6. HERTZ, H., "On the Equilibrium of Floating Elastic Slabs" (in German). Wiedemann's *Annalen der Physik und Chemie,* Vol. 22, pp. 449-455; also in *Gesammelte Werke* Vol. 1, pp. 288-294 (1884).
7. TELLER, L. W., and E. C. SUTHERLAND, "The Structural Design of Concrete Pavements." *Pub. Roads,* Vol. 16, Nos 8, 9, 10, pp 145-158, 169-197, 201-221, Vol. 23, No. 8, pp. 167-212 (1935, 1936, 1943).
8. SPANGLER, M. G , "Stresses in Concrete Pavement Slabs." *Proc. HRB,* Vol. 15, pp. 122-146 (1935).
9. SPANGLER, M. G., and F. E. LIGHTBURN, "Stresses in Concrete Pavement Slabs." *Proc. HRB,* Vol. 17, pp. 215-234 (1937).
10. KELLEY, E. F., "Application of the Results of Research to the Structural Design of Concrete Pavements." *Pub. Roads,* Vol. 20, No. 5, pp. 83-104 (1939).
11. BURMISTER, D. M., "The Theory of Stresses and Displacements in Layered Systems and Application to the Design of Airport Runways." *Proc. HRB,* Vol. 23, pp. 126-148 (1943).
12. ODEMARK, N , "Investigations as to the Elastic Properties of Soils and Design of Pavements According to the Theory of Elasticity" (in Swedish). *Meddelande No. 77,* Vaginstitut (1942).

13. PICKETT, G., and G. K. RAY, "Influence Charts for Concrete Pavements." *Trans. ASCE*, Vol. 116, pp. 49-73 (1951).
14. PELTIER, R., "Analysis of Rigid Pavements for Highways and Airports" (in French). *Revue Générale des Routes*, pp. 249-265 (Oct. 1952).
15. JEUFFROY, G., and J. BACHELEZ, "Note on a Method of Analysis for Pavements." *Proc. Intern. Conf on Struct. Design of Asphalt Pavements*, pp. 300-309, Ann Arbor (1962).
16. HOLL, D. L., "Thin Plates on Elastic Foundations." *Proc. Fifth Intern. Congress on Appl. Mech.*, pp. 71-74, Cambridge, Mass. (1938).
17. HOGG, A. H. A., "Equilibrium of a Thin Plate, Symmetrically Loaded, Resting on an Elastic Foundation of Infinite Depth." *Philosophical Mag.*, Vol. 25, pp. 576-582 (1938).
18. JOHANSEN, K. W , "Theory of Yield Lines" (in Danish) Dissertation, Gjellerup, Copenhagen (1943).
19. LOSBERG, A., "Design Methods for Structurally Reinforced Concrete Pavements " *Trans , Chalmers Univ. of Tech.*, No 250, 144 pp., Gothenburg (1961).
20. FOX, L., "Computation of Traffic Stresses in a Simple Road Structure." *Road Res. Paper No. 9*, Road Research Laboratory (England). H. M. Stat. Off., London (1948).
21. WINKLER, E., *Study of Elasticity and Strength* (in German). H Dominikus, Prague, pp. 182-184 (1867).
22. ZIMMERMAN, H., *Analysis of Railway Superstructure* (in German). Berlin (1888).
23. ENGESSER, F., "On Theory of Foundation Soil" (in German). *Zentralblatt der Bauverwaltung*, pp. 306-312 (1893).
24. GOLDBECK, A. T., and M. J. BUSSARD, "The Supporting Value of Soil as Influenced by the Bearing Area." *Pub. Roads*, Vol. 6, No 1, pp. 1-8 (1925).
25. TERZAGHI, K., "Soil Pressure and the Coefficient of Subgrade Reaction" (in German). *Osterreich. Bauzeitung*, No. 25 (1932).
26. BIOT, M. A , "Bending of an Infinite Beam on an Elastic Foundation " *Jour. Appl Mech., Trans. ASME*, Vol. 59, pp. A1-A7 (1937)
27. DE BEER, E. E., "Analysis of Beams Resting on Soil" (in French). *Ann. des Travaux Publics de Belgique*, Vol 101, pp. 393-418, 525-552, 653-691, 721-749 (1948).
28. CAQUOT, A., and J. KÉRISEL, *Treatise on Soil Mechanics* (in French). 3rd Ed., Gauthier-Villars, Paris (1956).
29. TERZAGHI, K., "Evaluation of Coefficients of Subgrade Reaction " *Geotechnique*, Vol. 5, pp. 297-326 (1955).
30. VESIĆ, A., "Bending of Beams Resting on Isotropic Elastic Solid." *Proc. ASCE, Jour. Eng. Mech. Div.*, Vol. 87, EM2, pp. 35-51 (1961).
31. VESIĆ, A., "Beams on Elastic Subgrade and the Winkler's Hypothesis." *Proc. Fifth Intern. Conf. on Soil Mechanics and Foundation Eng.*, Vol. I, pp. 845-850 (1961).
32. VESIĆ, A., and W. H. JOHNSON, "Model Studies of Beams Resting on a Silt Subgrade." *Proc. ASCE, Jour. Soil Mech. and Foundations Div.*, 89, SM1, p. 1 (1963).
33. TIMOSHENKO, S., and S. WOINOWSKY-KRIEGER, *Theory of Plates and Shells*. Ch. 8, McGraw-Hill (1959).
34. WESTERGAARD, H. M., "On Analysis of Slabs and Elastic Subgrade" (in Danish). *Ingeniören*, Vol. 32, pp. 513-524 (1923).
35. PICKETT, G., S. BADARUDDIN, and S. C. GANGULI, "Semi-Infinite Pavement Slab Supported by an Elastic Solid Subgrade." *Proc. First Congress Theor. Appl. Mechanics*, pp. 51-60, Kharagpur, India (1955).
36. PICKETT, G., and S. BADARUDDIN, "Influence Chart for Bending of a Semi-Infinite Pavement Slab." *Proc. Ninth Intern. Congress App. Mech.*, Vol. 6, pp. 396-402, Brussels (1956).
37. HOGG, A. H. A., "Equilibrium of a Thin Slab on an Elastic Foundation of Finite Depth." *Philosophical Mag.*, Vol. 35, pp 265-276 (1944)
38. VESIĆ, A , "The Validity of Layered Solid Theories for Flexible Pavements." *Proc. Intern. Conf. on Structural Design of Asphalt Pavements*, pp. 283-290, Ann Arbor, Mich. (1962).
39. "The AASHO Road Test." *HRB Spec. Rep. 61* (7 reports) (1961-1962).
    A. "History and Description of Project."
    B "Materials and Construction."
    C. "Traffic Operations and Pavement Maintenance."
    D. "Bridge Research."
    E. "Pavement Research."
    F. "Special Studies."
    G. "Summary Report."
40. HUDSON, W. R , and F. H. SCRIVNER, "AASHO Road Test Principal Relationships—Performance with Stress, Rigid Pavements. *HRB Spec. Rep. 73* (1962) pp. 227-241.
41. "Results of Modulus of Subgrade Reaction Determination at the AASHO Road Test Site by Means of Pavement Volumetric Displacement Tests." Ohio River Div Lab., Corps of Engineers, U.S. Army, Cincinnati, Ohio (1962).
42. SCRIVNER, F. H., "Structural Deterioration of Test Pavements· Rigid." *HRB Spec. Rep. 73* (1962) pp. 186-197.
43. VESIĆ, A S., and L. DOMASCHUK, "Theoretical Analysis of Structural Behavior of Road Test Flexible Pavements." *NCHRP Report 10* (1964).
44. FINN, F. N., "Asphalt Institute Discussion." (Conf. on the AASHO Road Test) *HRB Spec. Rep. 73* (1962) pp. 267-271.
45. SHOOK, J. F., and H. Y. FANG, "Cooperative Materials Testing Program at the AASHO Road Test." *HRB Spec. Rep. 66* (1961) pp. 59-102.
46. SEED, H. B., C. K. CHAN, and C. E. LEE, "Resilience Characteristics of Subgrade Soils and Their Relation to Fatigue Failures in Asphalt Pavements." *Proc. Intern. Conf. on Struct Design of Asphalt Pavements*, pp. 611-636 (1963).
47. COFFMAN, B. S., D. C. KRAFT, and J. TAMAYO, "A

Comparison of Calculated and Measured Deflections for the AASHO Road Test. *Proc. Assn. Asphalt Paving Tech.*, Vol. 33, pp 54-91 (1964).

48. SOWERS, G. F., "Stress, Bearing Capacity and Flexible Pavement Thickness Design Based on the AASHO Road Test and Georgia Pavement Evaluation Tests" *Report 6*, Project B-133, Engineering Exp Sta., Georgia Inst. of Technology, pp. 90 (1964).
49. NEWMARK, N M, "Numerical Methods of Analysis of Bars, Plates, and Elastic Bodies" *Numerical Methods of Analysis in Engineering* (L. E. Grinter, ed.). McMillan, pp. 138-168 (1949).
50. HUDSON, W. R., and H. MATLOCK, "Discontinuous Orthotropic Plates and Pavement Slabs." *Res. Report 56-6*, Center for Highway Research, Univ. of Texas (1966).
51. HUDSON, W. R, and H. MATLOCK, "Cracked Pavement Slabs with Nonuniform Support." *Proc. ASCE, Jour. Highway Div.*, Vol. 93, No. HW1, pp. 19-42 (1967)
52. SKOK, E L., and F. N. FINN, "Theoretical Concepts Applied to Asphalt Concrete Pavement Design" *Proc. Intern Conf. on Struct. Design of Asphalt Pavements*, Ann Arbor, pp. 412-440 (1962).

APPENDIX A

FINITE ELEMENT METHOD OF ANALYSIS OF SLABS RESTING ON SOIL

The classical differential equation of bending of a thin plate resting on an elastic subgrade is usually written in the form (*33*):

$$D\left(\frac{\partial^4 w}{\partial x^4} + 2\frac{\partial^4 w}{\partial x^2 \partial y^2} + \frac{\partial^4 w}{\partial y^4}\right) = q - p \qquad \text{(A-1)}$$

in which w is the deflection of the plate at any point (x,y); D is the flexural stiffness of the plate, given earlier (Eq 5); $q(x,y)$ is the external lateral unit load on the plate (positive downwards), and $p(x,y)$ is the reactive pressure of the subgrade. Assuming that the reactive pressure, p, is proportional to the deflection, w, at the same point (Winkler's hypothesis), Eq A-1 is transformed into

$$D\left(\frac{\partial^4 w}{\partial x^4} + 2\frac{\partial^4 w}{\partial x^2 \partial y^2} + \frac{\partial^4 w}{\partial y^4}\right) = q - k\,w \qquad \text{(A-2)}$$

Solutions of this equation can be obtained with reasonable effort by conventional methods as long as the slab and the subgrade are assumed to be continuous and homogeneous. However, pavement slabs often contain discontinuities such as joints and cracks and may possess only partial subgrade support It has been shown by Hudson and Matlock (*50, 51*) that the analysis of such slabs can conveniently be made by using a finite element approach, first suggested by Newmark (*49*).

All the slab analyses made in the present investigations have been based on such an approach and follow closely the method developed by Hudson and Matlock. The basic finite element model used is shown in Figure A-1. A typical nodal point is shown in Figure A-2. The axial deformability and the Poisson's effect of slab elements are represented by elastic blocks. The torsional stiffness of the elements is represented by torsion bars. It should be noted that the slab so conceived is of orthotropic behavior in any single element; however, there may be arbitrary differences in individual stiffnesses of different elements. The reaction of the subgrade is represented by elastic springs under nodal points The free-body diagram of a nodal point showing all the unknown internal forces of the system is shown in Figure A-3 Figure A-4 shows a plan view of the slab model with the numbering system used.

The equation of vertical equilibrium of a nodal point requires that

$$Q_{i,j} + V_{a,j}{}^{x} + V_{i,c}{}^{y} - V_{b,j}{}^{x} - V_{i,d}{}^{y} - S_{i,j}\,w_{i,j} = 0 \qquad \text{(A-3)}$$

The shearing forces, V, in this equation can be evaluated in terms of bending and twisting moments, which in turn can be expressed by their finite-difference equivalents in terms of deflections of adjacent points. After all transformations Eq. A-3 appears as a linear equation containing unknown deflections of 13 nodal points clustered in a rhomboidal array around the considered nodal point i,j:

$$\begin{aligned} &a_{i,j}\,w_{i,j-2} + b_{i,j}\,w_{i-1,j-1} + c_{i,j}\,w_{i,j-1} + d_{i,j}\,w_{i+1,j-1} \\ &+ e_{i,j}\,w_{i-2,j} + f_{i,j}\,w_{i+1,j} + g_{i,j}\,w_{i,j} + h_{i,j}\,w_{i+1,j} \\ &+ p_{i,j}\,w_{i+2,j} + q_{i,j}\,w_{i-1,j+1} + r_{i,j}\,w_{i,j+1} + s_{i,j}\,w_{i+1,j+1} \\ &+ t_{i,j}\,w_{i,j+2} = u_{i,j} \end{aligned} \qquad \text{(A-4)}$$

in which coefficients a through u are given by the following terms:

$$a_{i,j} = \frac{h_x}{h_y{}^3}\,(D^{y}{}_{i,j-1}) \qquad \text{(A-5)}$$

$$b_{i,j} = \frac{1}{h_x h_y}\,(\nu_{yx} D^{x}{}_{i-1,j} + \nu_{xy} D^{y}{}_{i,j-1} + C^{x}{}_{i,j} + C^{y}{}_{i,j}) \qquad \text{(A-6)}$$

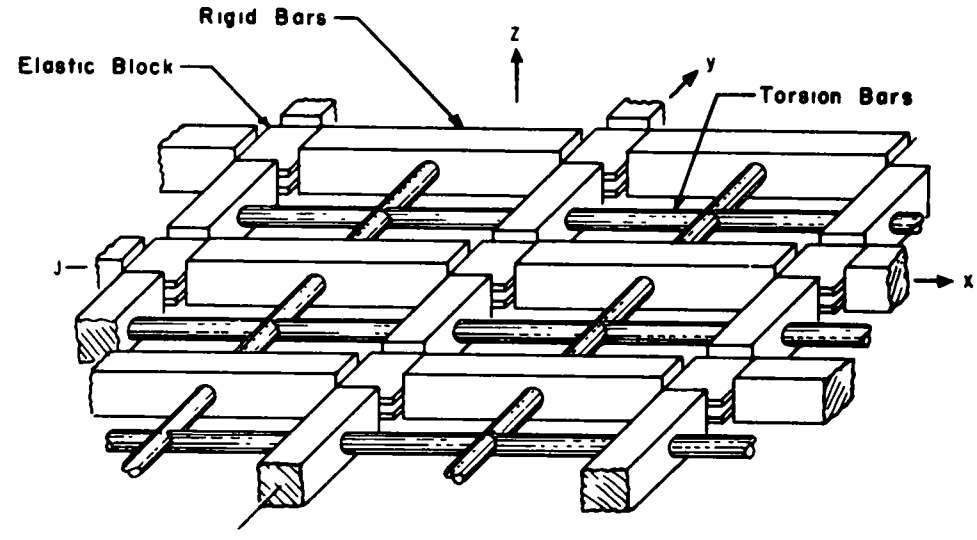

Figure A-1. Finite element model of a plate or slab (after Hudson and Matlock, 50).

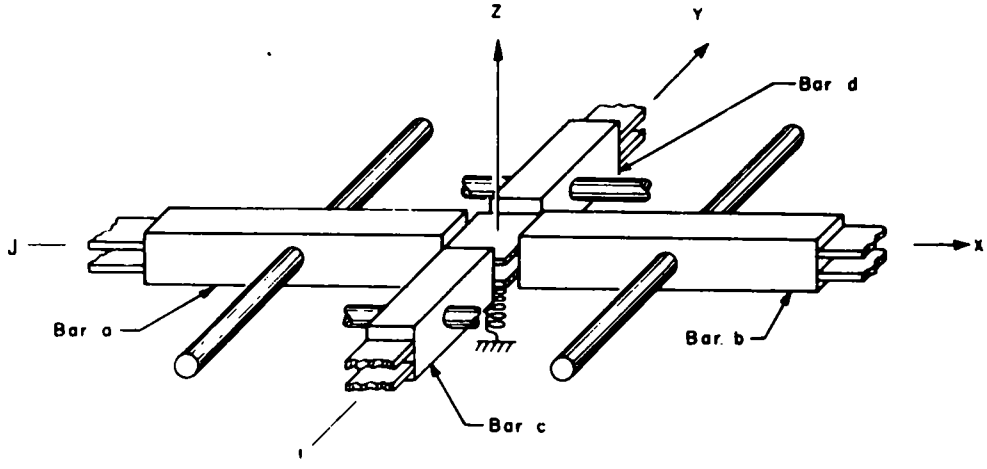

Figure A-2. Typical joint (i, j) taken from finite-element slab model (after Hudson and Matlock, 50)

$$c_{i,j} = -\frac{2h_x}{h_y^3}(D^{v}_{i,j-1} + D^{v}_{i,j}) - \frac{1}{h_x h_y}(2\nu_{yx}D^{x}_{i,j} + 2\nu_{xy}D^{v}_{i,j-1} + C^{x}_{i,j} + C^{x}_{i+1,j} + C^{v}_{i,j} + C^{v}_{i+1,j}) - \frac{P^{v}_{i,j}}{h_y} \quad \text{(A-7)}$$

$$d_{i,j} = \frac{1}{h_x h_y}(\nu_{yx}D^{x}_{i+1,j} + \nu_{xy}D^{v}_{i,j-1} + C^{x}_{i+1,j} + C^{v}_{i+1,j}) \quad \text{(A-8)}$$

$$e_{i,j} = \frac{h_x}{h_x^3}(D^{x}_{i-1,j}) \quad \text{(A-9)}$$

$$f_{i,j} = -\frac{2h_y}{h_x^3}(D^{x}_{i-1,j} + D^{x}_{i,j}) - \frac{1}{h_x h_y}(2\nu_{yx}D^{x}_{i-1,j} + 2\nu_{xy}D^{v}_{i,j} + C^{x}_{i,j} + C^{x}_{i,j+1} + C^{v}_{i,j} + C^{v}_{i,j+1}) - \frac{P^{x}_{i,j}}{h_x} \quad \text{(A-10)}$$

$$g_{i,j} = \frac{h_y}{h_x^3}(D^{x}_{i-1,j} + 4D^{x}_{i,j} + D^{x}_{i+1,j}) + \frac{h_x}{h_y^3}(D^{v}_{i,j-1} + 4D^{v}_{i,j} + D^{v}_{i,j+1}) + \frac{1}{h_x h_y}(4\nu_{yx}D^{x}_{i,j} + 4\nu_{xy}D^{v}_{i,j} + C^{x}_{i,j} + C^{x}_{i,j+1} + C^{x}_{i+1,j} + C^{x}_{i+1,j+1} + C^{v}_{i,j} + C^{v}_{i+1,j} + C^{v}_{i,j+1} + C^{v}_{i+1,j+1}) + \frac{1}{h_x}(P^{x}_{i,j} + P^{x}_{i+1,j}) + \frac{1}{h_y}(P^{v}_{i,j} + P^{v}_{i,j+1}) + S_{i,j} \quad \text{(A-11)}$$

$$h_{i,j} = -\frac{2h_y}{h_x^3}(D^{x}_{i,j} + D^{x}_{i+1,j}) - \frac{1}{h_x h_y}(2\nu_{yx}D^{x}_{i+1,j} + 2\nu_{xy}D^{v}_{i,j} + C^{x}_{i+1,j} + C^{x}_{i+1,j+1} + C^{v}_{i+1,j} + C^{v}_{i+1,j+1}) - \frac{P^{x}_{i+1,j}}{h_x} \quad \text{(A-12)}$$

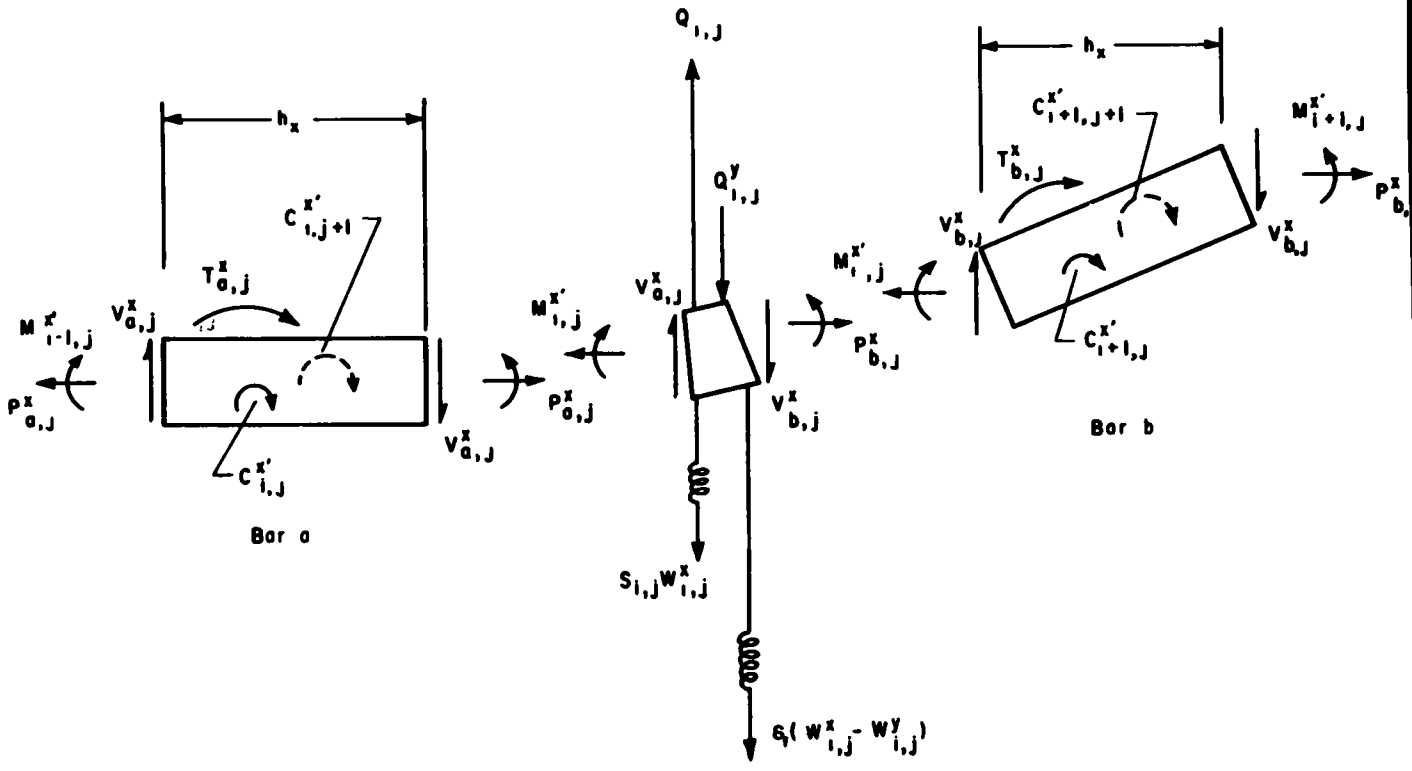

Figure A-3. Free body of slab mesh point (after Hudson and Matlock, 50).

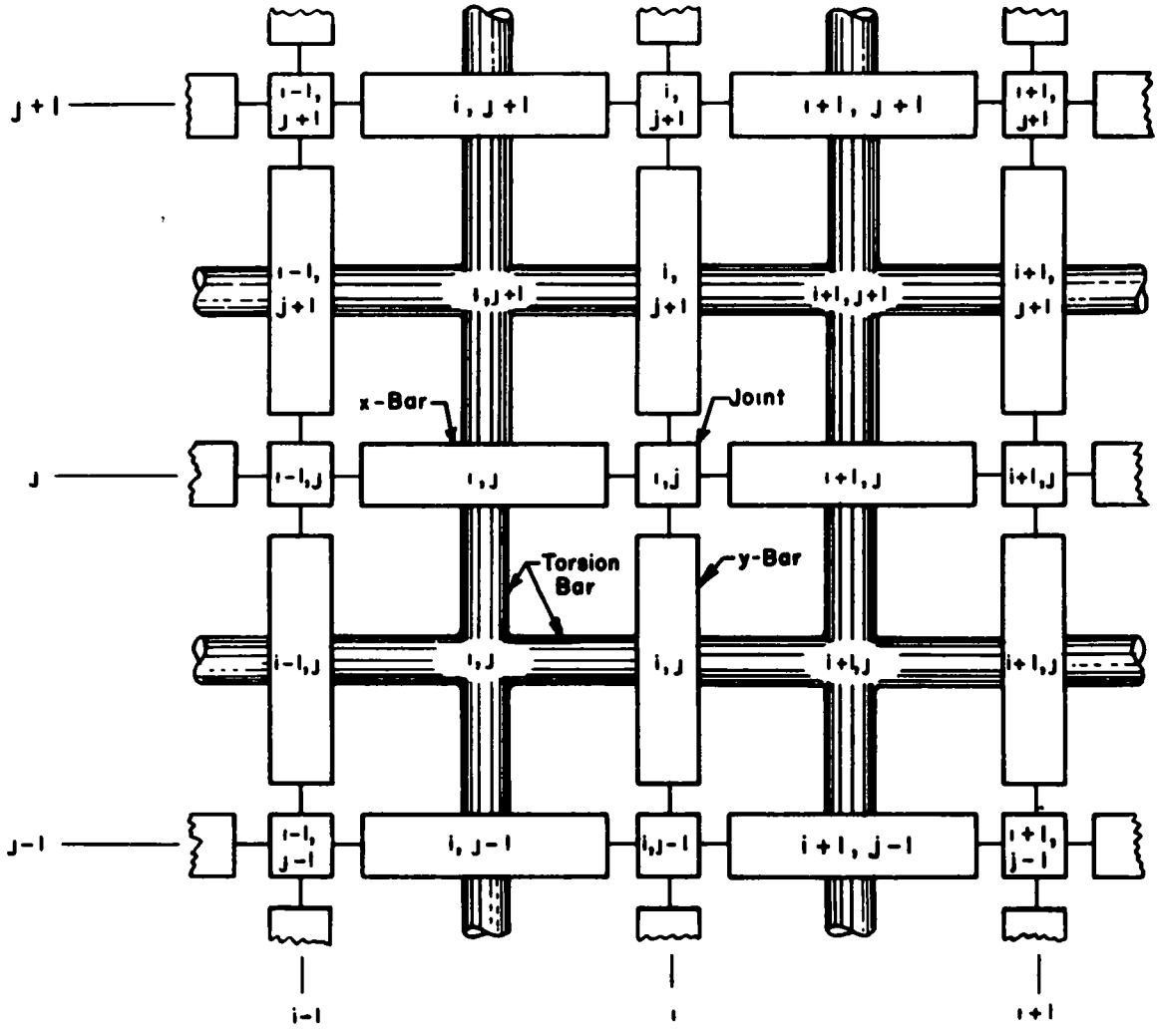

Figure A-4. Plan view of slab model showing all parts with generalized numbering system (after Hudson and Matlock, 50).

$$p_{i,j} = \frac{h_y}{h_x^3}\,(D^x{}_{i+1,j}) \tag{A-13}$$

$$q_{i,j} = \frac{1}{h_x h_y}\,(\nu_{yx} D^x{}_{i-1,j} + \nu_{xy} D^y{}_{i,j+1} + C^x{}_{i,j+1} + C^y{}_{i,j+1}) \tag{A-14}$$

$$r_{i,j} = -\frac{2h_x}{h_y^3}\,(D^y{}_{i,j} + D^y{}_{i,j+1}) - \frac{1}{h_x h_y}\,(2\nu_{yx} D^x{}_{i,j} + 2\nu_{xy} D^y{}_{i,j+1} + C^x{}_{i,j+1} + C^x{}_{i+1,j+1} + C^y{}_{i,j+1} + C^y{}_{i+1,j+1}) - \frac{P^y{}_{i,j+1}}{h_y} \tag{A-15}$$

$$s_{i,j} = \frac{1}{h_x h_y}\,(\nu_{yx} D^x{}_{i+1,j} + \nu_{xy} D^y{}_{i,j+1} + C^x{}_{i+1,j+1} + C^y{}_{i+1,j+1}) \tag{A-16}$$

$$t_{i,j} = \frac{h_x}{h_y^3}\,(D^y{}_{i,j+1}) \tag{A-17}$$

$$u_{i,j} = Q_{i,j} - \frac{1}{h_x}\,(T^x{}_{i,j} - T^x{}_{i+1,j}) - \frac{1}{h_y}\,(T^y{}_{i,j} - T^y{}_{i,j+1}) \tag{A-18}$$

The symbols in these equations are defined as follows:

- $C^x{}_{i,j}$ = torsional stiffness of the slab element i,j about the x axis (lb-in.);
- $C^y{}_{i,j}$ = torsional stiffness of the slab element i,j about the y axis (lb-in.);
- $D^x{}_{i,j}$ = flexural stiffness of the slab element i,j about the x axis (lb-in.);
- $D^y{}_{i,j}$ = flexural stiffness of the slab element i,j about the y axis (lb-in.);
- $Q_{i,j}$ = external load applied at point i,j;
- $S_{i,j}$ = subgrade reaction acting on the slab element i,j (lb/in.);
- $P^x{}_{i,j}$ = axial load acting on the slab element in the x direction (lb),
- $P^y{}_{i,j}$ = axial load acting on the slab element in the y direction (lb);
- h_x = distance between adjacent nodal points in the x direction (in.);
- h_y = distance between adjacent nodal points in the y direction (in.);
- ν_{xy} = Poisson's ratio indicating strains in the x direction due to stress in the y direction; and
- ν_{yx} = Poisson's ratio indicating strains in the y direction due to stress in the x direction.

The unknown deflections, w_{ij}, at nodal points can be determined by solving the appropriate system of linear equations such as Eq. A-4. This can be done with reasonable ease by using an alternating-direction-recursive technique described by Hudson and Matlock (*50*). The program for the present analysis, written in FORTRAN 2 language, is based on consideration of two 12 × 15-ft pavement slab panels connected by a doweled joint (Fig. A-5). With 595 nodal points spaced 1 ft in both x and y directions, the program requires storage of about 120,000 words. All the computations were performed on the IBM 360 system of the Triangle Universities Computation Center in Durham, N.C.

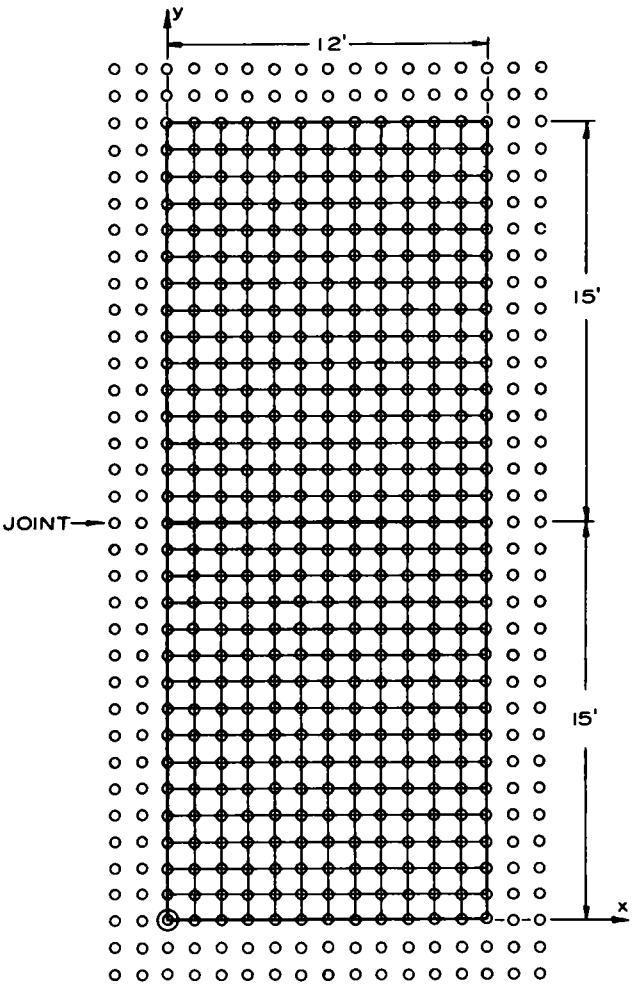

Figure A-5. Plan of slab panel used for computations.

Published reports of the

NATIONAL COOPERATIVE HIGHWAY RESEARCH PROGRAM

are available from.

Highway Research Board
National Academy of Sciences
2101 Constitution Avenue
Washington, D.C. 20418

Rep. No.	*Title*
—*	A Critical Review of Literature Treating Methods of Identifying Aggregates Subject to Destructive Volume Change When Frozen in Concrete and a Proposed Program of Research—Intermediate Report (Proj. 4-3(2)), 81 p., $1.80
1	Evaluation of Methods of Replacement of Deteriorated Concrete in Structures (Proj. 6-8), 56 p, $2.80
2	An Introduction to Guidelines for Satellite Studies of Pavement Performance (Proj 1-1), 19 p, $1.80
2A	Guidelines for Satellite Studies of Pavement Performance, 85 p. + 9 figs, 26 tables, 4 app, $3.00
3	Improved Criteria for Traffic Signals at Individual Intersections—Interim Report (Proj. 3-5), 36 p, $1.60
4	Non-Chemical Methods of Snow and Ice Control on Highway Structures (Proj 6-2), 74 p., $3.20
5	Effects of Different Methods of Stockpiling Aggregates—Interim Report (Proj. 10-3), 48 p., $2.00
6	Means of Locating and Communicating with Disabled Vehicles—Interim Report (Proj. 3-4), 56 p. $3 20
7	Comparison of Different Methods of Measuring Pavement Condition—Interim Report (Proj. 1-2), 29 p, $1 80
8	Synthetic Aggregates for Highway Construction (Proj. 4-4), 13 p., $1 00
9	Traffic Surveillance and Means of Communicating with Drivers—Interim Report (Proj. 3-2), 28 p, $1 60
10	Theoretical Analysis of Structural Behavior of Road Test Flexible Pavements (Proj 1-4), 31 p, $2 80
11	Effect of Control Devices on Traffic Operations—Interim Report (Proj. 3-6), 107 p., $5 80
12	Identification of Aggregates Causing Poor Concrete Performance When Frozen—Interim Report (Proj 4-3(1)), 47 p, $3.00
13	Running Cost of Motor Vehicles as Affected by Highway Design—Interim Report (Proj. 2-5), 43 p, $2.80
14	Density and Moisture Content Measurements by Nuclear Methods—Interim Report (Proj 10-5), 32 p., $3 00
15	Identification of Concrete Aggregates Exhibiting Frost Susceptibility—Interim Report (Proj. 4-3(2)), 66 p, $4.00
16	Protective Coatings to Prevent Deterioration of Concrete by Deicing Chemicals (Proj. 6-3), 21 p., $1.60
17	Development of Guidelines for Practical and Realistic Construction Specifications (Proj. 10-1), 109 p, $6.00
18	Community Consequences of Highway Improvement (Proj. 2-2), 37 p., $2.80
19	Economical and Effective Deicing Agents for Use on Highway Structures (Proj. 6-1), 19 p, $1.20
20	Economic Study of Roadway Lighting (Proj. 5-4), 77 p, $3.20
21	Detecting Variations in Load-Carrying Capacity of Flexible Pavements (Proj. 1-5), 30 p., $1.40
22	Factors Influencing Flexible Pavement Performance (Proj 1-3(2)), 69 p, $2.60
23	Methods for Reducing Corrosion of Reinforcing Steel (Proj. 6-4), 22 p., $1.40
24	Urban Travel Patterns for Airports, Shopping Centers, and Industrial Plants (Proj 7-1), 116 p., $5.20
25	Potential Uses of Sonic and Ultrasonic Devices in Highway Construction (Proj 10-7), 48 p, $2.00
26	Development of Uniform Procedures for Establishing Construction Equipment Rental Rates (Proj. 13-1), 33 p, $1.60
27	Physical Factors Influencing Resistance of Concrete to Deicing Agents (Proj. 6-5), 41 p., $2.00
28	Surveillance Methods and Ways and Means of Communicating with Drivers (Proj. 3-2), 66 p., $2.60
29	Digital-Computer-Controlled Traffic Signal System for a Small City (Proj. 3-2), 82 p., $4.00
30	Extension of AASHO Road Test Performance Concepts (Proj 1-4(2)), 33 p, $1.60
31	A Review of Transportation Aspects of Land-Use Control (Proj. 8-5), 41 p., $2.00
32	Improved Criteria for Traffic Signals at Individual Intersections (Proj. 3-5), 134 p., $5.00
33	Values of Time Savings of Commercial Vehicles (Proj. 2-4), 74 p, $3.60
34	Evaluation of Construction Control Procedures—Interim Report (Proj. 10-2), 117 p., $5.00
35	Prediction of Flexible Pavement Deflections from Laboratory Repeated-Load Tests (Proj. 1-3(3)), 117 p, $5.00
36	Highway Guardrails—A Review of Current Practice (Proj. 15-1), 33 p, $1.60
37	Tentative Skid-Resistance Requirements for Main Rural Highways (Proj. 1-7), 80 p., $3.60
38	Evaluation of Pavement Joint and Crack Sealing Materials and Practices (Proj. 9-3), 40 p., $2.00
39	Factors Involved in the Design of Asphaltic Pavement Surfaces (Proj. 1-8), 112 p., $5.00
40	Means of Locating Disabled or Stopped Vehicles (Proj. 3-4(1)), 40 p., $2.00
41	Effect of Control Devices on Traffic Operations (Proj. 3-6), 83 p., $3.60
42	Interstate Highway Maintenance Requirements and Unit Maintenance Expenditure Index (Proj. 14-1), 144 p., $5.60
43	Density and Moisture Content Measurements by Nuclear Methods (Proj. 10-5), 38 p., $2.00
44	Traffic Attraction of Rural Outdoor Recreational Areas (Proj. 7-2), 28 p., $1.40
45	Development of Improved Pavement Marking Materials—Laboratory Phase (Proj. 5-5), 24 p., $1.40
46	Effects of Different Methods of Stockpiling and Handling Aggregates (Proj 10-3), 102 p., $4.60
47	Accident Rates as Related to Design Elements of Rural Highways (Proj 2-3), 173 p., $6.40
48	Factors and Trends in Trip Lengths (Proj. 7-4), 70 p, $3 20
49	National Survey of Transportation Attitudes and Behavior—Phase I Summary Report (Proj. 20-4), 71 p., $3.20

* Highway Research Board Special Report 80

Rep. No. Title

50 Factors Influencing Safety at Highway-Rail Grade Crossings (Proj 3-8), 113 p., $5.20
51 Sensing and Communication Between Vehicles (Proj. 3-3), 105 p., $5.00
52 Measurement of Pavement Thickness by Rapid and Nondestructive Methods (Proj. 10-6), 82 p., $3.80
53 Multiple Use of Lands Within Highway Rights-of-Way (Proj. 7-6), 68 p., $3.20
54 Location, Selection, and Maintenance of Highway Guardrails and Median Barriers (Proj. 15-1(2)), 63 p., $2.60
55 Research Needs in Highway Transportation (Proj. 20-2), 66 p., $2.80
56 Scenic Easements—Legal, Administrative, and Valuation Problems and Procedures (Proj. 11-3), 174 p., $6.40
57 Factors Influencing Modal Trip Assignment (Proj. 8-2), 78 p., $3.20
58 Comparative Analysis of Traffic Assignment Techniques with Actual Highway Use (Proj. 7-5), 85 p., $3.60
59 Standard Measurements for Satellite Road Test Program (Proj. 1-6), 78 p., $3.20
60 Effects of Illumination on Operating Characteristics of Freeways (Proj. 5-2) 148 p., $6.00
61 Evaluation of Studded Tires—Performance Data and Pavement Wear Measurement (Proj. 1-9), 66 p., $3.00
62 Urban Travel Patterns for Hospitals, Universities, Office Buildings, and Capitols (Proj. 7-1), 144 p., $5.60
63 Economics of Design Standards for Low-Volume Rural Roads (Proj. 2-6), 93 p., $4.00
64 Motorists' Needs and Services on Interstate Highways (Proj. 7-7), 88 p., $3.60
65 One-Cycle Slow-Freeze Test for Evaluating Aggregate Performance in Frozen Concrete (Proj. 4-3(1)), 21 p., $1.40
66 Identification of Frost-Susceptible Particles in Concrete Aggregates (Proj. 4-3(2)), 62 p., $2.80
67 Relation of Asphalt Rheological Properties to Pavement Durability (Proj. 9-1), 45 p., $2.20
68 Application of Vehicle Operating Characteristics to Geometric Design and Traffic Operations (Proj. 3-10), 38 p., $2.00
69 Evaluation of Construction Control Procedures—Aggregate Gradation Variations and Effects (Proj. 10-2A), 58 p., $2.80
70 Social and Economic Factors Affecting Intercity Travel (Proj. 8-1), 68 p., $3.00
71 Analytical Study of Weighing Methods for Highway Vehicles in Motion (Proj. 7-3), 63 p., $2.80
72 Theory and Practice in Inverse Condemnation for Five Representative States (Proj. 11-2), 44 p., $2.20
73 Improved Criteria for Traffic Signal Systems on Urban Arterials (Proj. 3-5/1), 55 p., $2.80
74 Protective Coatings for Highway Structural Steel (Proj. 4-6), 64 p., $2.80
75 Effect of Highway Landscape Development on Nearby Property (Proj. 2-9), 82 p., $3.60
76 Detecting Seasonal Changes in Load-Carrying Capabilities of Flexible Pavements (Proj. 1-5(2)), 37 p., $2.00
77 Development of Design Criteria for Safer Luminaire Supports (Proj. 15-6), 82 p., $3.80

Rep. No. Title

78 Highway Noise—Measurement, Simulation, and Mixed Reactions (Proj. 3-7), 78 p., $3.20
79 Development of Improved Methods for Reduction of Traffic Accidents (Proj. 17-1), 163 p., $6.40
80 Oversize-Overweight Permit Operation on State Highways (Proj. 2-10), 120 p., $5.20
81 Moving Behavior and Residential Choice—A National Survey (Proj. 8-6), 129 p., $5.60
82 National Survey of Transportation Attitudes and Behavior—Phase II Analysis Report (Proj. 20-4), 89 p., $4.00
83 Distribution of Wheel Loads on Highway Bridges (Proj. 12-2), 56 p., $2.80
84 Analysis and Projection of Research on Traffic Surveillance, Communication, and Control (Proj. 3-9), 48 p., $2.40
85 Development of Formed-in-Place Wet Reflective Markers (Proj. 5-5), 28 p., $1.80
86 Tentative Service Requirements for Bridge Rail Systems (Proj. 12-8), 62 p., $3.20
87 Rules of Discovery and Disclosure in Highway Condemnation Proceedings (Proj. 11-1(5)), 28 p., $2.00
88 Recognition of Benefits to Remainder Property in Highway Valuation Cases (Proj. 11-1(2)), 24 p., $2.00
89 Factors, Trends, and Guidelines Related to Trip Length (Proj. 7-4), 59 p., $3.20
90 Protection of Steel in Prestressed Concrete Bridges (Proj. 12-5), 86 p., $4.00
91 Effects of Deicing Salts on Water Quality and Biota—Literature Review and Recommended Research (Proj. 16-1), 70 p., $3.20
92 Valuation and Condemnation of Special Purpose Properties (Proj. 11-1(6)), 47 p., $2.60
93 Guidelines for Medial and Marginal Access Control on Major Roadways (Proj. 3-13), 147 p., $6.20
94 Valuation and Condemnation Problems Involving Trade Fixtures (Proj. 11-1(9)), 22 p., $1.80
95 Highway Fog (Proj. 5-6), 48 p., $2.40
96 Strategies for the Evaluation of Alternative Transportation Plans (Proj. 8-4), 111 p., $5.40
97 Analysis of Structural Behavior of AASHO Road Test Rigid Pavements (Proj. 1-4(1)A), 35 p., $2.60

Synthesis of Highway Practice

1 Traffic Control for Freeway Maintenance (Proj. 20-5, Topic 1), 47 p., $2.20
2 Bridge Approach Design and Construction Practices (Proj. 20-5, Topic 2), 30 p., $2.00
3 Traffic-Safe and Hydraulically Efficient Drainage Practice (Proj. 20-5, Topic 4), 38 p., $2.20

THE NATIONAL ACADEMY OF SCIENCES is a private, honorary organization of more than 700 scientists and engineers elected on the basis of outstanding contributions to knowledge. Established by a Congressional Act of Incorporation signed by President Abraham Lincoln on March 3, 1863, and supported by private and public funds, the Academy works to further science and its use for the general welfare by bringing together the most qualified individuals to deal with scientific and technological problems of broad significance.

Under the terms of its Congressional charter, the Academy is also called upon to act as an official—yet independent—adviser to the Federal Government in any matter of science and technology. This provision accounts for the close ties that have always existed between the Academy and the Government, although the Academy is not a governmental agency and its activities are not limited to those on behalf of the Government.

THE NATIONAL ACADEMY OF ENGINEERING was established on December 5, 1964. On that date the Council of the National Academy of Sciences, under the authority of its Act of Incorporation, adopted Articles of Organization bringing the National Academy of Engineering into being, independent and autonomous in its organization and the election of its members, and closely coordinated with the National Academy of Sciences in its advisory activities. The two Academies join in the furtherance of science and engineering and share the responsibility of advising the Federal Government, upon request, on any subject of science or technology.

THE NATIONAL RESEARCH COUNCIL was organized as an agency of the National Academy of Sciences in 1916, at the request of President Wilson, to enable the broad community of U. S. scientists and engineers to associate their efforts with the limited membership of the Academy in service to science and the nation. Its members, who receive their appointments from the President of the National Academy of Sciences, are drawn from academic, industrial and government organizations throughout the country. The National Research Council serves both Academies in the discharge of their responsibilities.

Supported by private and public contributions, grants, and contracts, and voluntary contributions of time and effort by several thousand of the nation's leading scientists and engineers, the Academies and their Research Council thus work to serve the national interest, to foster the sound development of science and engineering, and to promote their effective application for the benefit of society.

THE DIVISION OF ENGINEERING is one of the eight major Divisions into which the National Research Council is organized for the conduct of its work. Its membership includes representatives of the nation's leading technical societies as well as a number of members-at-large. Its Chairman is appointed by the Council of the Academy of Sciences upon nomination by the Council of the Academy of Engineering.

THE HIGHWAY RESEARCH BOARD, organized November 11, 1920, as an agency of the Division of Engineering, is a cooperative organization of the highway technologists of America operating under the auspices of the National Research Council and with the support of the several highway departments, the Bureau of Public Roads, and many other organizations interested in the development of transportation. The purpose of the Board is to advance knowledge concerning the nature and performance of transportation systems, through the stimulation of research and dissemination of information derived therefrom.

HIGHWAY RESEARCH BOARD
NATIONAL ACADEMY OF SCIENCES—NATIONAL RESEARCH COUNCIL
2101 Constitution Avenue Washington, D. C. 20418

ADDRESS CORRECTION REQUESTED